Biochemical Pharmacology 82 (2011) 1110–1125

Contents lists available at ScienceDirect

Biochemical Pharmacology

journal homepage: www.elsevier.com/locate/biochempharm

Proteasome inhibitor MG132-induced apoptosis via ER stress-mediated apoptotic pathway and its potentiation by protein tyrosine kinase p56^{lck} in human Jurkat T cells

Hae Sun Park [a], Do Youn Jun [b], Cho Rong Han [a], Hyun Ju Woo [a], Young Ho Kim [a,*]

[a] Laboratory of Immunobiology, School of Life Science and Biotechnology, College of Natural Sciences, Kyungpook National University, Daegu 702-701, Republic of Korea
[b] Institute of Life Science and Biotechnology, Kyungpook National University, Daegu 702-701, Republic of Korea

ARTICLE INFO

Article history:
Received 7 May 2011
Accepted 18 July 2011
Available online 23 July 2011

Keywords:
Proteasome inhibitor
Apoptosis
ER stress
Mitochondria-dependent caspase cascade
p56^{lck}

ABSTRACT

Exposure of human Jurkat T cells to MG132 caused apoptosis along with upregulation of Grp78/BiP and CHOP/GADD153, activation of JNK and p38MAPK, activation of Bak, mitochondrial membrane potential ($\Delta\psi m$) loss, cytochrome *c* release, activation of caspase-12, -9, -3, -7, and -8, cleavage of Bid and PARP, and DNA fragmentation. However, these MG132-induced apoptotic events, with the exceptions of upregulation of Grp78/BiP and CHOP/GADD153 and activation of JNK and p38MAPK, were abrogated by overexpression of Bcl-xL. Pretreatment with the pan-caspase inhibitor z-VAD-fmk prevented MG132-induced apoptotic caspase cascade, but allowed upregulation of Grp78/BiP and CHOP/GADD153 levels, activation of JNK and p38MAPK, $\Delta\psi m$ loss, and cleavage of procaspase-9 (47 kDa) to active form (35 kDa). Further analysis using selective caspase inhibitors revealed that caspase-12 activation was required for activation of caspase-9 and -3 to the sufficient level for subsequent activation of caspase-7 and -8. MG132-induced cytotoxicity, apoptotic sub-G_1 peak, Bak activation, and $\Delta\psi m$ loss were markedly reduced by p38MAPK inhibitor, but not by JNK inhibitor. MG132-induced apoptotic changes, including upregulation of Grp78/BiP and CHOP/GADD153 levels, activation of caspase-12, p38MAPK and Bak, and mitochondria-dependent activation of caspase cascade were more significant in p56^{lck}-stable transfectant JCaM1.6/lck than in p56^{lck}-deficient JCaM1.6/vector. The cytotoxicity of MG132 toward p56^{lck}-positive Jurkat T cell clone was not affected by the Src-like kinase inhibitor PP2. These results demonstrated that MG132-induced apoptosis was caused by ER stress and subsequent activation of mitochondria-dependent caspase cascade, and that the presence of p56^{lck} enhances MG132-induced apoptosis by augmenting ER stress-mediated apoptotic events in Jurkat T cells.

1. Introduction

Proteasome is a large protease complex found in the cytoplasm and nucleus of mammalian cells, and it plays a critical role in the homeostatic control of a variety of cellular proteins by acting as the main non-lysosomal proteolytic system in the cells. Proteasome is known to catalyze a rapid degradation of structurally abnormal or misfolded proteins, and many essential regulatory proteins associated with external signal-induced cell activation and cell cycle progression, such as IkB, cyclin D2, cyclin D3, cyclin B, p53, and p27^{Kip1} [1]. The 26S proteasome recognizes ubiquitinated protein molecules and intakes them into a 20S proteolytic chamber for proteolytic degradation [2].

Since the proteasome inhibitor-induced suppression of the function of the ubiquitin–proteasome system appeared to lower cell proliferation and selectively induced apoptosis in actively proliferating cells [3], and since the proteasome inhibitor could block angiogenesis [4], the proteasome inhibitors have been examined as potential antineoplastic agents against various cancer cells *in vitro* and *in vivo*, including breast cancer, melanoma, lung cancer, lymphoma, and glioma cells [5–8]. As a mechanism associated with proteasome inhibitor-induced apoptosis, alteration in the level of cell cycle regulatory proteins including p27^{Kip1}, p21^{Cip1}, p16^{Ink4}, Mdm2, and p53, which led to growth-arrest at the G_1 phase and induction of apoptosis, has been implicated [9,10]. In addition, the activation of multiple caspases and the release of mitochondrial cytochrome *c* into cytoplasm have been observed during proteasome inhibitor-induced apoptosis [8]. Recently, it has been shown that proteasome inhibitor MG132-induced apoptosis of osteosarcoma cells is associated with growth-arrest at the G_2/M and activation of caspase-8 in the absence of activation of caspase-9 and -3 [11]. Since proteasome is part of the endoplasmic reticulum (ER)-associated machinery for protein degradation (ERAD) that removes unfolded and misfolded proteins from the

* Corresponding author. Tel.: +82 53 950 5378; fax: +82 53 955 5522.
E-mail address: ykim@knu.ac.kr (Y.H. Kim).

0006-2952/$ – see front matter © 2011 Elsevier Inc. All rights reserved.
doi:10.1016/j.bcp.2011.07.085

ER [12,13], it is likely that proteasome inhibition may cause the accumulation of unfolded and misfolded proteins in the ER and thus results in ER stress, which activates the unfold protein response (UPR). This UPR appears to induce apoptosis via the mitochondria-dependent and mitochondria-independent pathways involving C/EBP homologous protein/growth arrest- and DNA damage-inducible gene 153 (CHOP/GADD153), stress kinases such as c-Jun N-terminal kinase (JNK) and p38 mitogen-activated protein kinase (p38MAPK), and caspase-4 and -9 [14]. Although these previous results have indicated that disturbance of the cell cycle, ER stress, mitochondrial cytochrome *c* release, and activation of multiple caspases are involved in the proteasome inhibitor-induced apoptosis in tumors, their interrelations and the sequence for caspase cascade for the induction of proteasome inhibitor-induced apoptosis still remain obscure.

A protein tyrosine kinase (PTK) $p56^{lck}$ is a typical non-receptor PTK of the Src-family and is expressed almost exclusively in T cells [15]. The $p56^{lck}$ not only plays an important role in transducing TCR-mediated activation signal via interaction with cytoplasmic regions of CD4 and CD8 coreceptor molecules but it also relays the G_1/S-transition signal from the IL-2 receptor, indicating critical roles of $p56^{lck}$ for T-cell activation and proliferation. The importance of $p56^{lck}$ for T-cell propagation was initially indicated by virtue of its overexpression, resulting from retroviral insertion into the lck locus in two Moloney murine leukemia virus-induced lymphoid tumors [16]. In addition to the typical role of $p56^{lck}$ in T-cell propagation, $p56^{lck}$ is known to be involved in FasL expression during activation-induced T cell apoptosis [17] and Fas-mediated death signaling pathway leading to Bid cleavage and mitochondrial cytochrome *c* release [18]. Although these previous studies suggest that $p56^{lck}$ is associated with activation-induced T-cell apoptosis mainly via its role in upregulating FasL expression and its contribution to Fas-signaling pathway, several recent studies have indicated a direct requirement of $p56^{lck}$ for certain types of apoptosis induced by ionizing radiation, ceramide, rosmarinic acid, doxorubicin-, paclitaxel-, or 5-fluorouracil, through modulating the mitochondria-dependent apoptotic signaling pathway [19–23]. On the other hand, a $p56^{lck}$-deficient murine helper T cell clone resulting from $p56^{lck}$-specific antisense RNA expression was hypersusceptible to apoptosis when activated through TCR [24]. The phenylalanine analog para-fluorophenylalanine-induced apoptosis was more significant in $p56^{lck}$-deficient Jurkat T cells than in $p56^{lck}$-positive Jurkat T cells by increasing mitochondrial cytochrome *c* release and resultant activation of caspase cascade [25]. These previous data have suggested that $p56^{lck}$ plays a role in T-cell apoptosis as a pro-apoptotic or anti-apoptotic modulator and might be differential depending on initial triggers provoking apoptosis, but the precise mechanism has not been completely understood.

In the present study, to understand the mechanism underlying the apoptosis induced by the proteasome inhibitor and its modulation by protein tyrosine kinase $p56^{lck}$, we investigated the apoptotic signaling pathway provoked by MG132 in human acute leukemia Jurkat T cells, with focusing on ER-stress-mediated activation of JNK, p38MAPK, and caspase-12, and mitochondria-dependent caspase pathway. In addition, we investigated the effect of anti-apoptotic protein Bcl-xL on MG132-induced apoptosis. The results demonstrated that MG132-induced apoptosis was mediated by activation of p38MAPK, Bak, and mitochondria-dependent caspase cascade including caspase-9, -3, -7, and -8, in which ER stress-mediated activation of caspase-12 was crucial for the reciprocal activation of caspase-9 and -3. Our results also indicated that both ER stress-mediated activation of p38MAPK and caspase-12 and subsequent mitochondrial cytochrome *c* release were augmented in the presence of $p56^{lck}$ in Jurkat T cells.

2. Materials and methods

2.1. Reagents, antibodies, and cells

The proteasome inhibitor MG132 was purchased from Sigma Chemical (St. Louis, MO, USA). An ECL Western blotting kit was obtained from Amersham (Arlington Heights, IL, USA). Anti-cytochrome *c*, anti-Fas, and anti-FasL were purchased from Pharmingen (San Diego, CA, USA). Anti-phospho-JNK, anti-JNK1, anti-Grp78/BiP, anti-CHOP/GADD153, anti-caspase-3, anti-poly (ADP-ribose) polymerase (PARP), anti-Bax, anti-$p56^{lck}$, anti-Bcl-xL, anti-Bcl-2, and anti-β-actin were purchased from Santa Cruz Biotechnology (Santa Cruz, CA, USA). Anti-phospho-p38MAPK, anti-p38MAPK, anti-caspase-8, anti-caspase-9, anti-caspase-7, anti-Bad, anti-Bid, anti-phospho-$p56^{lck}$ (Tyr-505), and anti-phospho-$p56^{lck}$ (Tyr-416) were purchased from Cell Signaling Technology (Beverly, MA, USA). Anti-caspase-12 was obtained from BD Sciences (Chicago, IL, USA), and anti-BAG3 was purchased from Abcam (Cambridge, UK). The broad-range caspase inhibitor z-VAD-fmk, caspase-8 inhibitor z-IETD-fmk, anti-Bak (Ab-1), anti-Bax (6A7), JNK inhibitor SP600125, and the Src-like kinase inhibitor PP2 were obtained from Calbiochem (San Diego, CA, USA). The caspase-9 inhibitor z-LEHD-fmk and the caspase-3 inhibitor z-DEVD-fmk were obtained from BD Sciences, and the caspase-12 inhibitor z-ATAD-fmk and the caspase-4 inhibitor z-LEVD-fmk were obtained from Biovision (Mountain View, CA, USA). The p38MAPK inhibitor SB202190 was purchased from Biomol (Plymouth Meeting, PA, USA). Annexin V-FITC apoptosis kit was purchased from Clontech (Takara Bio Inc., Shiga, Japan). Human acute leukemia Jurkat T cell line E6.1, Jurkat T cell clone A3, and FADD-deficient Jurkat T cell clone I2.1 were purchased from ATCC (Manassas, VA, USA). Human acute leukemia Jurkat T cell clones J/Neo and J/Bcl-xL were provided by Dr. Dennis Taub (Gerontology Research Center, NIA/NIH, Baltimore, MD, USA). $p56^{lck}$-Stable transfectant JCaM1.6/lck and $p56^{lck}$-deficient JCaM1.6/vector were supplied from Dr. Arthur Weiss (University of California, San Francisco, CA, USA). Jurkat T cells were maintained in RPMI 1640 (Life Technologies, Gaithersburg, MD, USA) containing 10% FBS, 20 mM HEPES (pH 7.0), 5×10^{-5} M β-mercaptoethanol, and 100 μg/ml gentamycin. For the culture of J/Neo cells, J/Bcl-xL cells, JCaM1.6/lck, and JCaM1.6/vector, G418 (A.G. Scientific Inc., San Diego, CA, USA) was added to RPMI 1640 medium at a concentration of 400 μg/ml.

2.2. Cytotoxicity assay

The cytotoxic effect of MG132 on Jurkat T cells was analyzed by MTT assay. Briefly, cells (5×10^4) were added to the serial dilution of MG132 in 96-well plates. At 20 h after incubation, 50 μl of MTT solution (1.1 mg/ml) was added to each well and incubated for an additional 4 h. After centrifugation, the supernatant was removed from each well, and then 150 μl of DMSO was added to dissolve the colored formazan crystal produced from MTT. OD values of the solutions were measured at 540 nm by a plate reader.

2.3. DNA fragmentation analysis

Apoptotic DNA fragmentation induced in Jurkat T cells following MG132 treatment was determined by Triton X-100 lysis methods using 1.2% agarose gel electrophoresis as previously described [26].

2.4. Flow cytometric analysis

Flow cytometric analysis of the cell cycle of Jurkat T cells exposure to MG132 was performed as described elsewhere [26].

The extent of necrosis was detected with Annexin V-FITC apoptosis kit (Clontech, Takara Bio Inc., Shiga, Japan) as previously described [27]. Briefly, cells (5×10^5) were washed with 1× binding buffer and then incubated with Annexin V-FITC and propidium iodide (PI) for 15 min before being analyzed by flow cytometry.

Changes in the mitochondrial membrane potential ($\Delta\psi m$) following treatment with MG132 were measured after staining with 3,3′-dihexyloxacarbocyanine iodide ($DiOC_6$) [28]. After treatment with MG132, the cells were harvested and incubated with PBS containing 50 nM $DiOC_6$ for 1 min at 37 °C prior to flow cytometric analysis.

Activation of Bak and Bax following treatment with MG132 was measured by flow cytometry as previously described [23]. Briefly, cells (1×10^6) were washed with PBS and fixed in PBS/1.0% paraformaldehyde on ice for 30 min. Cells were then washed three times in PBS/1% FCS. Staining with conformation-specific antibodies against Bak (Ab-1) and Bax (6A7) was performed with a proper dilution of individual antibodies in 100 μl staining buffer (PBS, 500 μg/ml digitonin). Then, cells were washed and resuspended in 100 μl staining buffer containing Alexafluor 488-labeled goat anti-mouse IgG. The conformational changes of Bak and Bax were measured by flow cytometry.

2.5. Preparation of cell lysate and Western blot analysis

Cellular lysates were prepared by suspending 5×10^6 Jurkat T cells in 200 μl of lysis buffer (137 mM NaCl, 15 mM EGTA, 1 mM sodium orthovanadate, 15 mM $MgCl_2$, 0.1% Triton X-100, 25 mM MOPS, 2.5 μg/ml proteinase inhibitor E-64, and pH 7.2). The cells were disrupted by sonication and extracted at 4 °C for 30 min. An equivalent amount of protein lysate (20 μg) was electrophoresed on 4–12% SDS gradient polyacrylamide gel with MOPS buffer and then electrotransferred to Immobilon-P membranes. Detection of each protein was performed using an ECL Western blotting kit according to the manufacturer's instructions.

2.6. Detection of mitochondrial cytochrome c in cytosolic protein extracts

To assess mitochondrial cytochrome *c* release in Jurkat T cells following MG132 treatment, cytosolic protein extracts were obtained as described elsewhere [27]. The cytosolic extracts free of mitochondria were analyzed for cytochrome *c* by Western blotting.

2.7. Determination of caspase activity

Caspase-12 activity was assayed by using the Caspase-12 Fluorometric Assay Kit (Biovision, Mountain View, CA, USA), and caspase-3 activity was assayed by using the Caspase-3 Colorimetric Activity Assay Kits (Chemicon International Inc., Temecula, CA, USA) according to the manufacturer's protocols, as described elsewhere [29]. An equal number of cells (5×10^6) from each sample were treated with Cell Lysis Buffer on ice for 10 min, and centrifuged at 10,000 × *g* for 10 min. The supernatant (~150 μg of protein) was incubated with each caspase substrate (ATAD-FMC for caspase-12, and DEVD-pNA for caspase-3) at 37 °C for 1 h. For an *in vitro* caspase-12 inhibition assay, the cell lysate (150 μg of protein) prepared from Jurkat T cells treated with 2.5 μM MG132 for 12 h was added to various concentrations (0.1 μM, 0.5 μM, 1 μM, and 4 μM) of the caspase-12 inhibitor z-ATAD-fmk. After these mixtures were incubated at room temperature for 30 min to allow the z-ATAD-fmk to react with caspase-12, the substrate ATAD-FMC for caspase-12 was added to determine residual caspase-12 activity. Under the same conditions, to test for cross-reactivity of the caspase-12 inhibitor z-ATAD-fmk toward caspase-3 activity, the substrate DEVD-pNA for caspase-3 was added. Following the addition of the substrates, the reaction mixture was incubated at 37 °C for 1 h. The caspase-12 activity was measured by a fluorometer equipped with a 400-nm excitation filter and a 510-nm emission filter. The caspase-3 activity was measured by a microplate reader at 405 nm.

2.8. Statistical analysis

Unless otherwise indicated, each result in this work is representative of at least three separate experiments. Values represent the mean ± standard deviation (SD) of these experiments. The statistical significance was calculated with a Student's *t*-test. *P* values less than 0.05 were considered significant.

3. Results

3.1. Apoptogenic effect of MG132 on Jurkat T cell clone E6.1

To investigate the cytotoxic effect of MG132 on Jurkat T cells, cell viability after treatment with MG132 at various concentrations ranging from 0.63 μM to 2.5 μM for 12 h was determined by MTT assay. As shown in Fig. 1A, the cell viability declined in a dose-dependent manner. Although the cell viability in the presence of 0.63 μM MG132 remained at the level of 91%, the cell viability in the presence of 1.25 μM and 2.5 μM MG132 appeared to be 73% and 37%, respectively, indicating that the IC_{50} value of MG132 was 2.1 μM. The apoptotic DNA fragmentation began to be detected at a concentration of 1.25 μM and appeared to increase in a dose-dependent manner, in accordance with the decline in cell viability, indicating that MG132 possesses apoptogenic activity and induces apoptotic DNA fragmentation in a dose-dependent manner (Fig. 1B). Under these conditions, flow cytometric analysis also exhibited the accumulation of apoptotic sub-G_1 cells following treatment with MG132 (Fig. 1C). To examine the involvement of the mitochondrial apoptotic pathway in the apoptotic effect of MG132, the mitochondrial membrane potential ($\Delta\psi m$) loss of the cells treated with MG132 was measured by $DiOC_6$ staining. When the $\Delta\psi m$ loss was visualized as a reduction in the fluorescence signal in the FL1 channel, the ratio of negative fluorescence in E6.1 cells treated with MG132 at concentrations of 0.63 μM, 1.25 μM, and 2.5 μM were 4.3%, 19.3%, and 49.9%, respectively (Fig. 1D), demonstrating that MG132 could reduce $\Delta\psi m$ in a dose-dependent manner. To examine whether necrosis accompanied the apoptogenic activity of MG132, the cells treated with MG132 were analyzed by Annexin V-FITC and PI staining. The treatment of cells with MG132 caused an enhancement in the levels of early apoptotic cells stained only with Annexin V-FITC, and late apoptotic cells stained with both Annexin V-FITC and PI, whereas the necrotic cells stained only with PI were barely detected, indicating that the cytotoxic effect exerted by MG132 on Jurkat T cells was mainly attributable to induced apoptosis, but not to necrosis (Fig. 1E). These results indicated that the cytotoxic effect of MG132 on Jurkat T cells was attributable to mitochondrial damage and subsequent induction of apoptosis without necrosis.

3.2. Involvement of mitochondrial cytochrome c-mediated activation of caspase cascade, and ER stress-mediated activation of JNK, p38MAPK, and caspase-12 in MG132-induced apoptosis in Jurkat T cell clone E6.1

To examine that the pro-apoptotic action of cytochrome *c* released from mitochondria was involved in the MG132-induced apoptotic signaling pathway in Jurkat T cells, we investigated mitochondrial cytochrome *c* release into cytoplasm and resultant activation of caspase cascade including caspase-9 and -3, leading

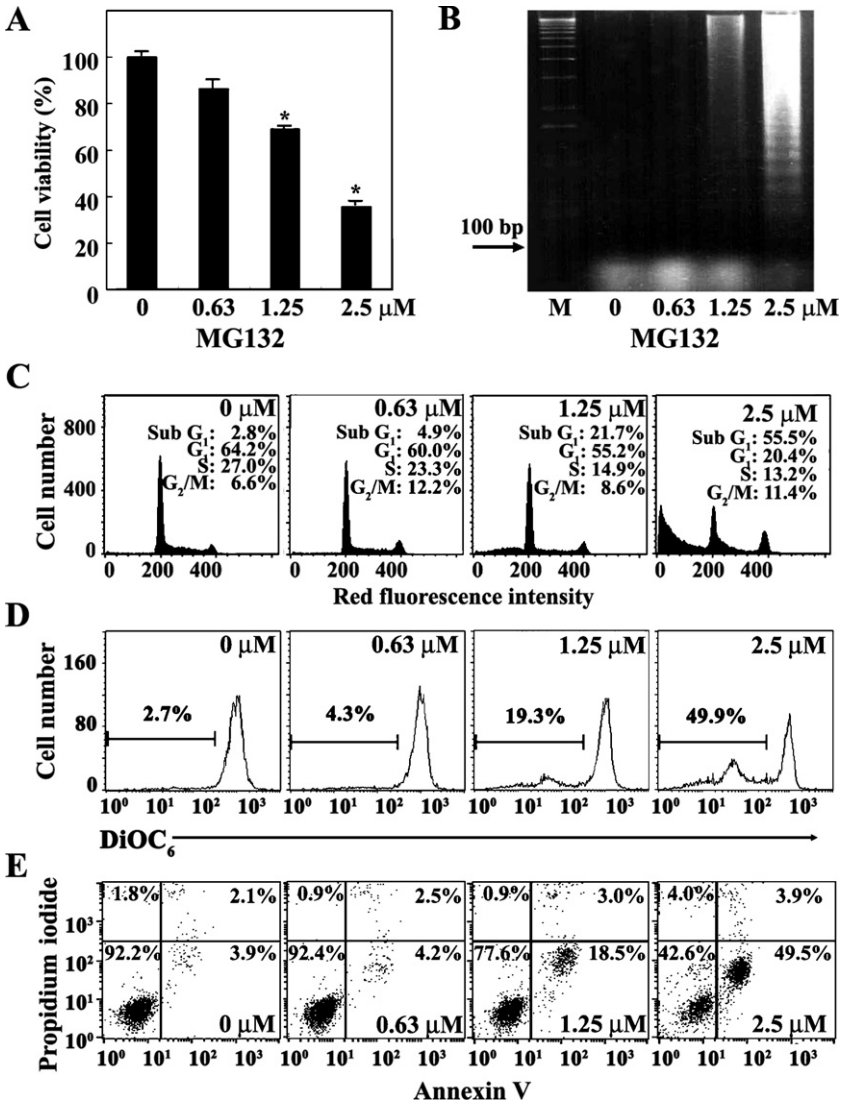

Fig. 1. Effect of MG132 on cell viability (A), apoptotic DNA fragmentation (B), cell cycle distribution (C), mitochondrial membrane potential ($\Delta\psi m$) loss (D), and apoptotic cell death (E) in Jurkat T cell clone E6.1. The cells (7.5×10^4) were incubated with indicated concentrations of MG132 in a 96-well plate for 12 h and the final 4 h were incubated with MTT. The cells were sequentially processed to assess the colored formazan crystal produced from MTT as an index of cell viability. Each value is expressed as mean ± SD ($n = 3$ with three replicates per independent experiment). *$P < 0.05$ compared to control. Equivalent cultures were prepared and processed for apoptotic DNA fragmentation analysis by Triton X-100 lysis methods using 1.2% agarose gel electrophoresis. The cell cycle distribution was determined on an equal number of cells (2×10^4) by flow cytometric analysis of PI staining. The $\Delta\psi m$ loss and the apoptotic cells were determined by flow cytometric analysis of $DiOC_6$ staining, and Annexin V-FITC and PI staining, respectively.

to degradation of PARP. Although there was no detectable cytochrome *c* in the cytosolic fraction of continuously growing Jurkat T cells, the level of cytosolic cytochrome *c* increased by MG132 (1.25–2.5 μM) in a dose-dependent manner (Fig. 2A). At the same time, the level of β-actin remained constant, indicating the equivalent loading of the cell lysate in each lane for Western blot analysis. Along with the mitochondrial cytochrome *c* release, caspase-9 activation that proceeded via proteolytic cleavage of procaspase-9 (47 kDa) into the active forms (37/35 kDa) was detected (Fig. 2B). The activation of caspase-3 through proteolytic cleavage of 32-kDa procaspase-3 into the 17-kDa active form as well as the activation of procaspase-7 (35 kDa) into the active form (20 kDa) was also detected. As a downstream target of active caspase-3 and -7 during induction of apoptosis, PARP has been reported to be cleaved into two fragments [30]. The cleavage of PARP was detected along with activation of caspase-3 and -7 in the presence of 1.25–2.5 μM MG132. To examine whether ER stress-mediated apoptotic events were provoked as the upstream signals in MG132-induced mitochondrial cytochrome *c* release and activation of caspase cascade, the activation of c-Jun N-terminal kinase (JNK) and p38 mitogen-activated protein kinase (p38MAPK), caspase-12 and -8, and the upregulation of glucose-regulated protein 78 (Grp78)/BiP and C/EBP homologous protein/growth arrest- and DNA damage-inducible gene 153 (CHOP/GADD153), all of which are known to be as the ER stress-mediated events [14,27,31–34], were also investigated by Western blot analysis. In the presence of MG132 (1.25–2.5 μM), the phosphorylation of JNK increased significantly without a change in the level of total JNK1 protein. Along with the JNK phosphorylation, the c-Jun appeared to be phosphorylated at Ser-63 residue, which is known to be catalyzed by JNK [35], suggesting that the phosphorylated JNK was enzymatically active enough to phosphorylate c-Jun. The phosphorylation of p38MAPK was also enhanced in a manner similar to the JNK phosphorylation, reflecting concurrent activation of JNK and p38MAPK following exposure to MG132. Under these conditions, the activation of Bak,

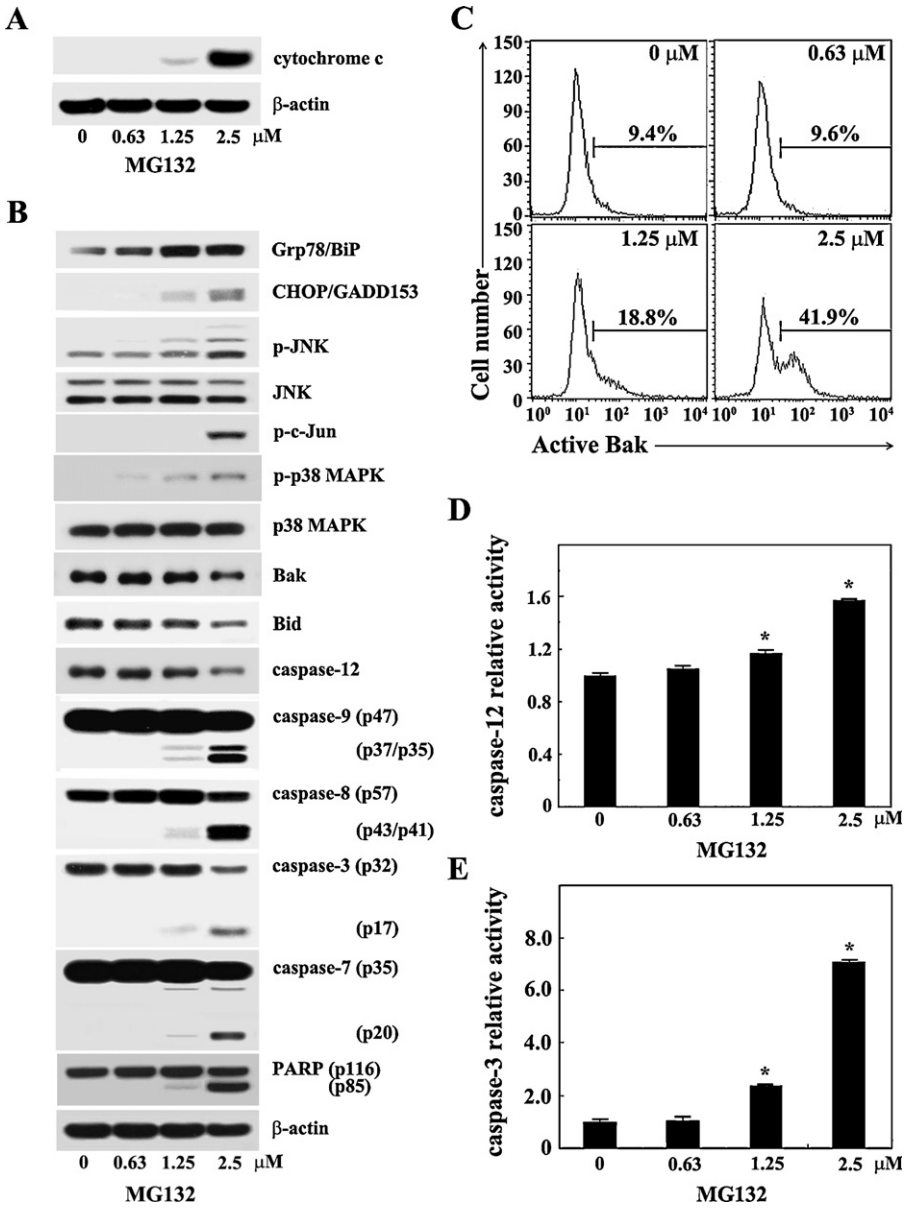

Fig. 2. Western blot analysis of mitochondrial cytochrome *c* release and β-actin (A), and Grp78/BiP, CHOP/GADD153, phospho-JNK, JNK1, phospho-c-Jun, phospho-p38MAPK, p38MAPK, Bak, Bid, caspase-12, -9, -3, -8, and -7, cleavage of PARP, and β-actin (B), flow cytometric analysis of Bak activation (C), and *in vitro* activity assay for caspase-12 (D) and caspase-3 (E) in Jurkat T cells (clone E6.1) after treatment with MG132 (0.63–2.5 μM). The cells (~5×10^6 cells) were incubated at a density of 5×10^5/ml with indicated concentrations of MG132 for 12 h and prepared for mitochondria-free cytosolic extracts or cell lysates. Western blot analysis, flow cytometric analysis of Bak activation, and the enzymic activity assay of caspase-12 or caspase-3 were performed as described in Section 2. Each value is expressed as mean ± SD ($n = 3$ with three replicates per independent experiment). $^*P < 0.05$ compared to control. A representative study is shown and two additional experiments yielded similar results.

as evidenced by its N-terminal conformational change, was detected (Fig. 2C). Whereas the level of procaspase-12 (55 kDa) appeared to remain constant, the activation of caspase-8 through proteolytic cleavage of proenzyme (57 kDa) into active forms (43/41 kDa) was significantly enhanced. In addition, the level of Bid protein (22 kDa), which was previously degraded by active caspase-8 to generate the truncated Bid (tBid, 15 kDa) causing $\Delta\psi$m loss and cytochrome *c* release [36,37], appeared to decrease. An enhancement in the levels of Grp78/BiP and CHOP/GADD153 was also detected in Jurkat T cells following exposure to MG132. Since the anti-caspase-12 employed for Western blot analysis in this study is known to recognize the procaspase-12 but not the cleaved form of caspase-12, we further evaluated *in vitro* caspase-12 activity to confirm MG132-induced caspase-12 activation in Jurkat T cells. As shown in Fig. 2D, the caspase-12 activity appeared to increase in a dose-dependent manner in Jurkat T cells. At the same time, the caspase-3 activity was enhanced in accordance with the results of Western blot analysis of MG132-induced caspase-3 activation (Fig. 2E). These *in vitro* caspase activity assays confirmed that MG132-induced apoptosis of Jurkat T cells was accompanied by caspase-12 activation. Since procaspase-12 and procaspase-8 are activated in response to ER stress [27,32,33], and since JNK and p38MAPK activated by ER stress can be translocated to mitochondria and contribute to Bak activation to provoke cytochrome *c* release [14,31,34], these previous and current results raised the possibility that the ER stress-mediated apoptotic pathways such as the activations of JNK, p38MAPK, caspase-12 and -8 might be involved in MG132-induced apoptosis as the upstream events for mitochondrial cytochrome *c* release and subsequent activation of caspase-9 and -3.

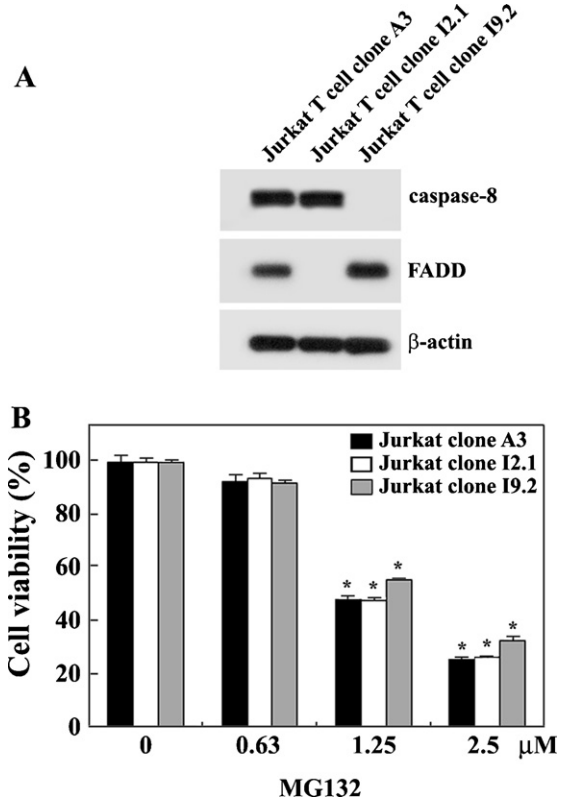

Fig. 3. Western blot analysis of caspase-8, FADD, and β-actin (A), and the effect of MG132 on cell viability (B) in wild-type Jurkat T cells (clone A3), FADD-deficient Jurkat T cells (clone I2.1), or caspase-8-deficient Jurkat T cells (clone I9.2). Equivalent amounts of individual cell lysates were electrophoresed on 4–12% SDS gradient polyacrylamide gels and electrotransferred to Immobilon-P membranes. Western analysis was performed as described in Section 2. A3 cells, I2.1 cells or I9.2 cells were incubated at a density of 7.5×10^4 cells per well with indicated concentrations of MG132 in a 96-well plate. After 8 h, an MTT assay was performed to assess cell viability. Each value is expressed as mean ± SD ($n = 3$ with three replicates per independent experiment). $^*P < 0.05$ compared to control.

To investigate an involvement of Fas/FasL system in MG132-induced apoptosis in Jurkat T cells, we compared the cytotoxic effect of MG132 on FADD-positive wild-type Jurkat T cells (clone A3) with those on FADD-deficient Jurkat T cells (clone I2.1) and caspase-8-deficient Jurkat T cells (clone I9.2), both of which were previously refractory to Fas-mediated apoptosis [38]. Jurkat clones exhibited a similar sensitivity to the cytotoxicity of MG132, regardless of the FADD- or caspase-8-deficiency (Fig. 3A and B). These results indicated that the MG132-induced apoptosis of Jurkat T cells was not initiated by the interaction of Fas with FasL, but by ER stress- and mitochondria-mediated activation of multiple caspases including caspase-12, -9, -8, -7, and -3, leading to PARP degradation. These results also suggested that the activation of caspase-8 and resultant cleavage of Bid into tBid might not be crucial for MG132-induced apoptosis.

3.3. Protective effect of anti-apoptotic protein Bcl-xL on MG132-induced apoptosis in Jurkat T cells

To examine whether these MG132-induced apoptotic events are crucial to apoptotic cell death, we decided to take advantage of the anti-apoptotic protein Bcl-xL that could protect cells from apoptosis by blocking both cytochrome *c* release from mitochondria and ER stress-mediated activation of caspase-12 and -8, resulting in the prevention of both mitochondria-dependent and -independent apoptotic pathways [27,39,40]. When the effect of the overexpression of Bcl-xL on the cytotoxicity of MG132 was investigated by employing Jurkat T cells transfected with *Bcl-xL* gene (J/Bcl-xL) and Jurkat T cells transfected with vector (J/Neo), the viability of J/Neo cells in the presence of 0.63 μM, 1.25 μM, and 2.5 μM MG132 was 87.2%, 59.0%, and 27.5%, whereas that of J/Bcl-xL cells was 96.1%, 95.4%, and 87.6%, respectively, indicating the protective effect of Bcl-xL on the cytotoxicity of MG132 (Fig. 4A). Under these conditions, MG132 (1.25–2.5 μM) could induce apoptotic DNA fragmentation in J/Neo cells in a dose-dependent manner, but it failed to induce the DNA fragmentation in J/Bcl-xL cells (Fig. 4B). Similarly, the flow cytometric analysis showed that the level of apoptotic sub-G_1 cells increased in J/Neo cells treated with MG132 (1.25–2.5 μM), whereas the apoptotic sub-G_1 cells were not detected in J/Bcl-xL cells treated with MG132 (Fig. 4C). When the Δψm loss of J/Neo cells treated with MG132 was measured by $DiOC_6$ staining, the ratio of negative fluorescence in the cells treated with MG132 at concentrations of 0.63 μM, 1.25 μM, and 2.5 μM were 4.0%, 33.7%, and 64.3%, respectively (Fig. 4D). However, MG132 failed to induce Δψm loss in J/Bcl-xL cells. These results demonstrated that MG132 caused Δψm loss and apoptotic DNA fragmentation in a dose-dependent manner by a conserved apoptogenic mechanism, which could be targeted by the anti-apoptotic role of Bcl-xL, and suggested that MG132-mediated cytotoxicity was mainly due to induced apoptosis.

Western blot analysis further revealed that although mitochondrial cytochrome *c* release into cytosol was induced dose-dependently in J/Neo cells treated with MG132 (1.25–2.5 μM), it was prevented in J/Bcl-xL cells (Fig. 5A). Along with mitochondrial cytochrome *c* release, the activation of caspase-9, -3, and -8, Bid cleavage, and PARP degradation was induced in J/Neo cells, but these apoptotic events were abrogated in J/Bcl-xL cells (Fig. 5B). Under these conditions, while MG132-induced upregulation in the levels of Grp78/BiP and CHOP/GADD153, and activation of JNK and p38MAPK were sustained or slightly enhanced in J/Bcl-xL cells, MG132-induced activation of caspase-12, which was evaluated by the *in vitro* caspase-12 activity assay, as well as MG132-induced activation of Bak appeared to be abrogated in J/Bcl-xL cells (Fig. 5C and D). In accordance with the results of Western blot analysis, the *in vitro* caspase-3 activity assay also showed that MG132-induced activation of caspase-3 could be completely blocked in J/Bcl-xL cells (Fig. 5E). These *in vitro* caspase activity assays demonstrated that MG132-induced activation of caspase-12 and -3 was negatively regulated by Bcl-xL. Consequently, these results indicated that the mitochondria-dependent activation of caspase cascade, which could be blocked by Bcl-xL, was crucial for MG132-induced apoptosis. These results also demonstrated that among the ER stress-associated apoptotic events, which occurred as upstream events of mitochondria-dependent caspase cascade, only the caspase-12 activation was susceptible to anti-apoptotic role of Bcl-xL.

3.4. Effect of various caspase inhibitors, JNK inhibitor, and p38MAPK inhibitor on MG132-induced apoptosis in Jurkat T cells

To elucidate further the MG132-induced death signaling pathways, we investigated the effect of caspase-9 inhibitor (z-LEHD-fmk) [41], caspase-3 inhibitor (z-DEVD-fmk) [42], pan-caspase inhibitor (z-VAD-fmk) [43], caspase-4 inhibitor (z-LEVD-fmk) [44], and caspase-12 inhibitor (z-ATAD-fmk) [45] on MG132-induced apoptotic events in Jurkat T cells. After pretreatment with each inhibitor for 2 h, the cells were exposed to 2.5 μM MG132 for 12 h. Although apoptotic sub-G_1 peak was barely or not detectable in continuously growing Jurkat T cells, it increased to the level of 40.0% in the presence of 2.5 μM MG132 for 12 h (Fig. 6A). The MG132-induced sub-G_1 peak was abrogated by z-LEHD-fmk, z-

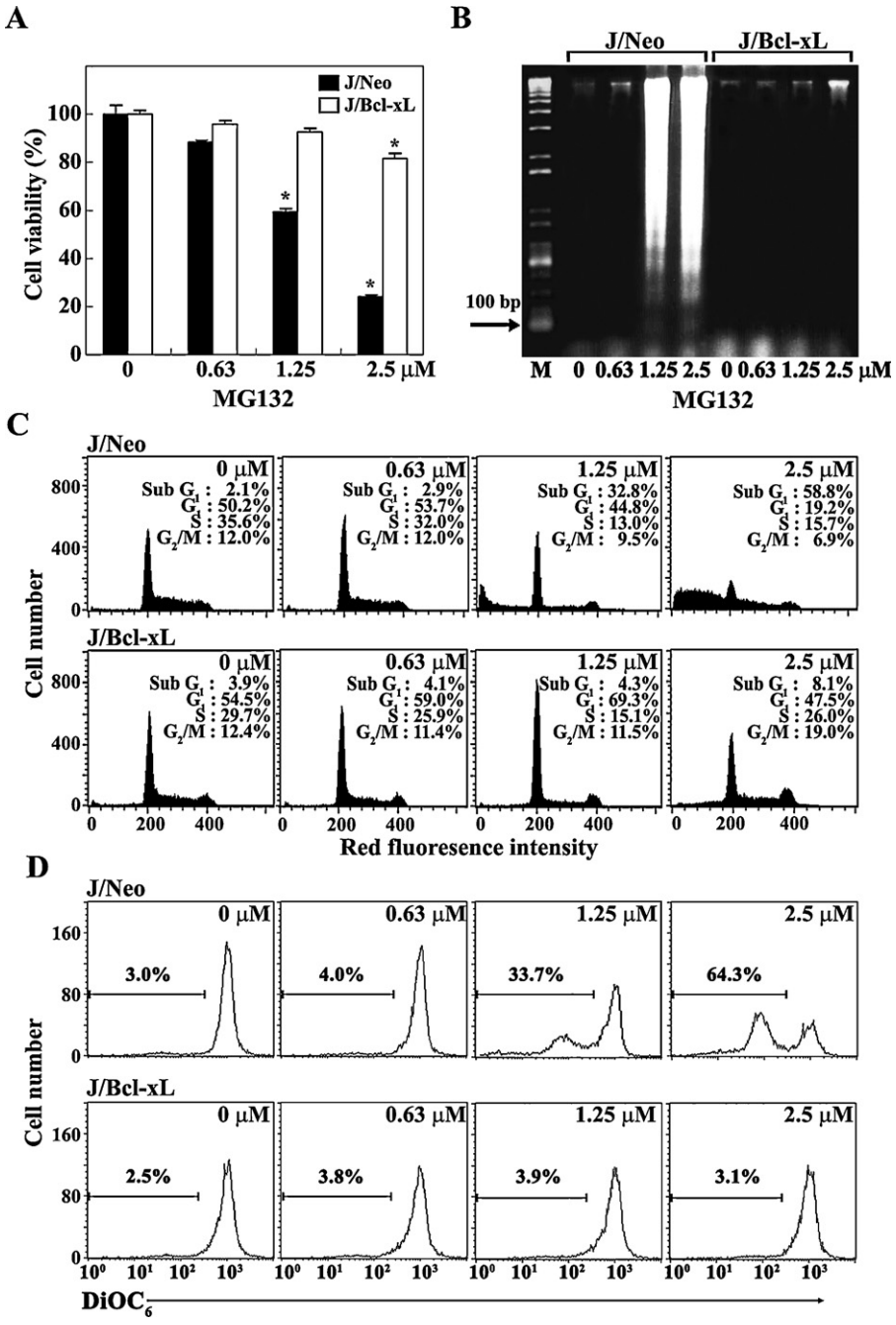

Fig. 4. Effect of Bcl-xL on MG132-induced cytotoxicity (A), apoptotic DNA fragmentation (B), apoptotic change in the cell cycle distribution (C), and $\Delta\psi m$ loss (D) in Jurkat T cells. Jurkat T cells overexpressing Bcl-xL (J/Bcl-xL) and control (J/Neo) cells were incubated at a density of 7.5×10^4/well with various concentrations of MG132 in a 96-well plate. After 8 h, an MTT assay was performed to determine cell viability. Each value is expressed as mean ± SD ($n = 3$ with three replicates per independent experiment). $^*P < 0.05$ compared to control. Equivalent cultures were prepared and processed for apoptotic DNA fragmentation analysis by Triton X-100 lysis methods using 1.2% agarose gel electrophoresis. The cell cycle distribution was determined on an equal number of cells (2×10^4) by flow cytometric analysis of PI staining. The $\Delta\psi m$ was determined by flow cytometric analysis of $DiOC_6$ staining.

DEVD-fmk, z-VAD-fmk, or z-ATAD-fmk, whereas the sub-G_1 peak was not reduced by z-LEVD-fmk. Under these conditions, none of these caspase inhibitors could prevent MG132-induced $\Delta\psi m$ loss of the cells, demonstrating that MG132-induced $\Delta\psi m$ loss was upstream of the caspase cascade (Fig. 6B). These results also suggested that the individual activities of caspase-12, -9, and -3 were crucial for MG132-induced apoptosis in Jurkat T cells, but the caspase-4 activity was required to a lesser extent.

As shown in Fig. 7A, Western blot analysis revealed that in the presence of z-VAD-fmk, MG132-induced apoptotic events such as activation of caspase-3, -7, and -8, cleavage of Bid, and degradation of PARP were completely blocked. This allowed the cleavage of 47 kDa procaspase-9 into 35 kDa active caspase-9 at a comparable level to that of the MG132-treated control cells. However, the generation of 37 kDa active caspase-9 was barely detected. These results exclude the possible involvement of caspase-8 activation as an initial signal provoking the mitochondrial cytochrome *c* release in MG132-induced apoptosis. In addition, MG132-induced phosphorylation of JNK and p38MAPK was induced at a slightly enhanced level in the presence of z-VAD-fmk, indicating that the activation of JNK and p38MAPK was upstream of the caspase cascade required for the induced apoptosis. The presence of either

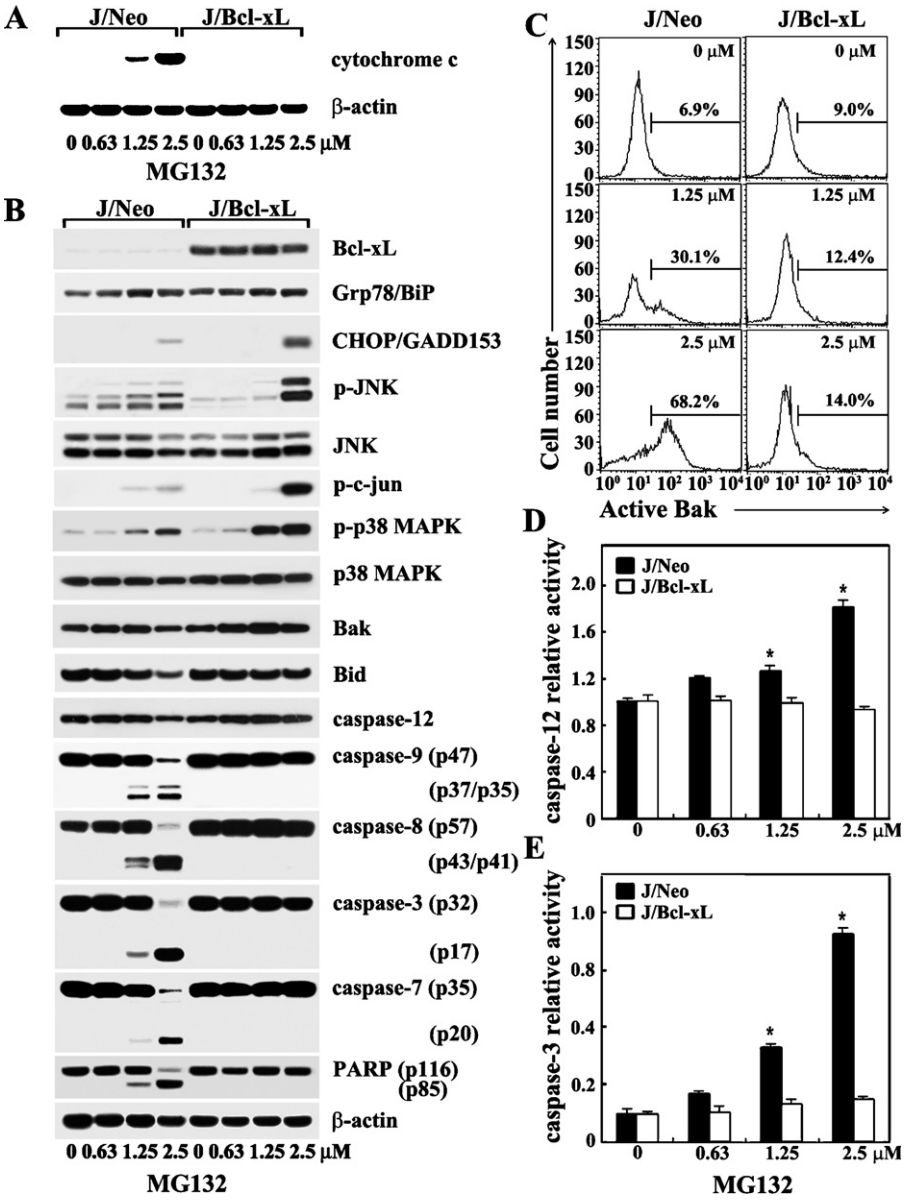

Fig. 5. Western blot analysis of mitochondrial cytochrome *c* release and β-actin (A), and Bcl-xL, Grp78/BiP, CHOP/GADD153, phospho-JNK, JNK1, phospho-c-Jun, phospho-p38MAPK, p38MAPK, Bak, Bid, caspase-12, -9, -3, -8, and -7, and cleavage of PARP (B), flow cytometric analysis of Bak activation (C), *in vitro* activity assay for caspase-12 (D), and caspase-3 (E) in Jurkat T cells transfected with empty vector (J/Neo) or Bcl-xL-expression vector (J/Bcl-xL) after treatment with MG132. The cells (~5×10^6 cells) were incubated at a density of 5×10^5/ml with indicated concentrations of MG132 for 12 h and prepared for mitochondria-free cytosolic extracts or cell lysates. Western blot analysis, flow cytometric analysis of Bak activation, and the enzymic activity assay of caspase-12 or caspase-3 were performed as described in Section 2. Each value is expressed as mean ± SD ($n = 3$ with three replicates per independent experiment). $^*P < 0.05$ compared to control. A representative study is shown and two additional experiments yielded similar results.

z-LEHD-fmk or z-DEVD-fmk caused not only a complete prevention of MG132-induced activation of caspase-7 and -8 and degradation of PARP but also a significant reduction to a barely detectable level of 37 kDa active caspase-9 with no generation of 17 kDa active caspase-3. At the same time, 35 kDa active caspase-9 was generated at a similar level to that of the MG132-treated control cells, along with generation of 19 kDa active caspase-3. Recently, it has been reported that the proteolytic cleavage of procaspase-9 (47 kDa) within the apoptosome yields 35/12 kDa active caspase-9 in order to cleave procaspase-3 (32 kDa) into active caspase-3 (20 kDa), and the subsequent feedback cleavage of procaspase-9 by 20 kDa active caspase-3 generates 37/10 kDa active caspase-9, which can cleave not only 20 kDa active caspase-3 into 17 kDa active caspase-3 but also 35 kDa procaspase-7 into 20 kDa active caspase-7 [46–49]. These previous and current results indicated that the activation of caspase-9 and -3 was upstream of the activation of caspase-7 and -8. The presence of z-ATAD-fmk completely blocked MG132-induced activation of caspase-7 and -8 with a significant reduction in the level of 37 kDa active caspase-9 and degradation of PARP. The presence of z-LEVD-fmk partially suppressed MG132-induced activation of caspase-7 and -8, but exerted no suppressive effect on activation of caspase-9 and degradation of PARP. Only 20 kDa active caspase-3 was produced from 32 kDa procaspase-3 in the presence of z-ATAD-fmk, whereas both the 20 kDa active form and the much lower level of 17 kDa active form of caspase-3 were concurrently generated in the presence of z-LEVD-fmk. Like z-VAD-fmk, none of the individual caspase inhibitors tested could suppress MG132-induced upregulation in the levels of Grp78/BiP and CHOP/GADD153, and activation of JNK and p38MAPK. In order to

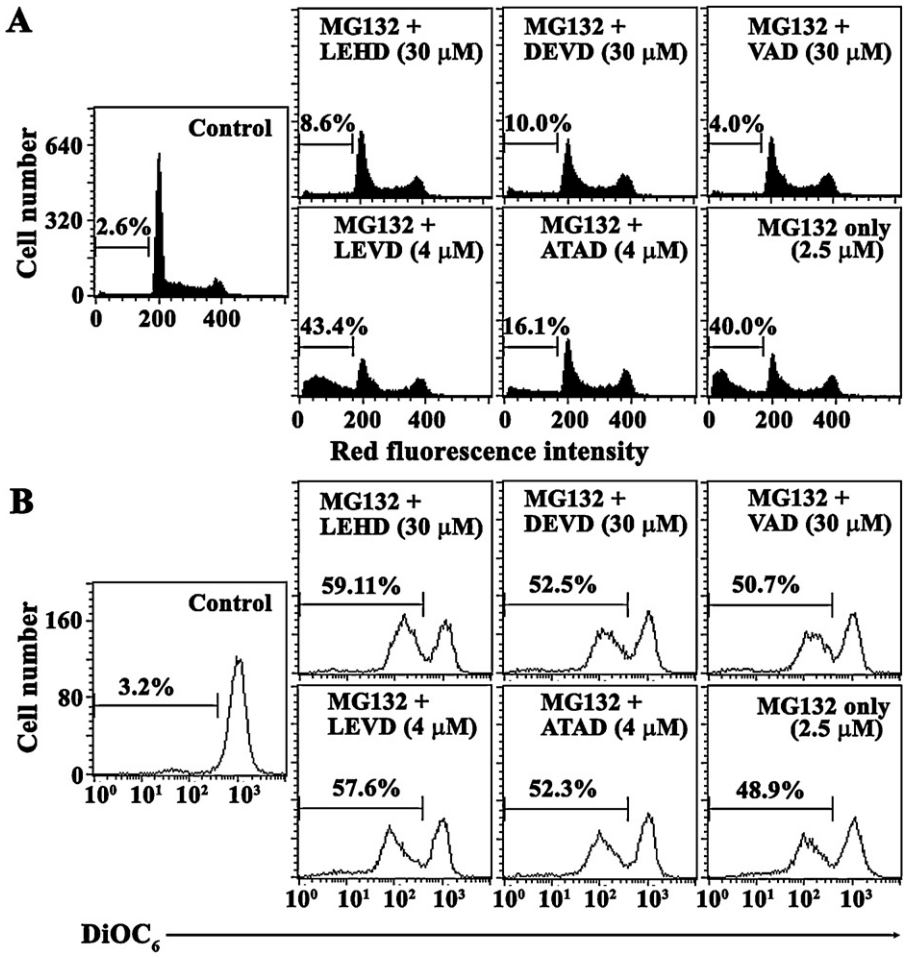

Fig. 6. Change in the cell cycle distribution (A) and $\Delta\psi m$ (B) in Jurkat T cells (clone E6.1) after treatment with 2.5 μM MG132 in the presence of 30 μM z-LEHD-fmk, 30 μM z-DEVD-fmk, 30 μM z-VAD-fmk, 4 μM z-LEVD-fmk, or 4 μM z-ATAD-fmk. The cells (5×10^5/ml) were preincubated with the individual caspase inhibitors for 2 h and then treated with 2.5 μM MG132 for 12 h. The cell cycle distribution was determined on an equal number of cells (2×10^4) by flow cytometric analysis of PI staining. The $\Delta\psi m$ was measured by flow cytometric analysis of $DiOC_6$ staining.

examine the inhibitory activity and specificity of z-ATAD-fmk toward the caspase-12, we investigated the inhibitory effect of various concentrations (0.5, 1.0, and 4.0 μM) of z-ATAD-fmk on the caspase-12 activity or the caspase-3 activity using the lysate of Jurkat T cells treated with 2.5 μM MG132 for 12 h as the enzyme solution. As shown in Fig. 7B, the caspase-12 activity was inhibited by z-ATAD-fmk in a dose-dependent manner with an inhibition of ~48% at concentrations of 1–4 μM, whereas the caspase-3 activity exhibited an inhibition of 10.5%, indicating the specificity of z-ATAD-fmk (1–4 μM) toward the caspase-12 in Jurkat T cells treated with MG132. These results indicated that the MG132-induced apoptotic signaling pathway was mediated by the mitochondria-dependent activation of caspase-9 and -3, where ER stress-mediated caspase-12 activation was required for its proper progression, leading to the activation of caspase-7 and -8. These results also indicated that MG132-induced activation of JNK and p38MAPK, which could be mediated by ER stress, was an upstream event of the mitochondria-dependent activation of caspase cascade.

To elucidate further the role of JNK and p38MAPK in MG132-induced death signaling pathway, leading to apoptosis in Jurkat T cells, we investigated the effect of JNK inhibitor (SP600125) or p38MAPK inhibitor (SB202190) on MG132-induced apoptotic events in Jurkat T cells. After pretreatment with either SP600125 at concentrations of 10 μM, 20 μM and 40 μM or SB202190 at concentrations of 25 μM, 50 μM, and 75 μM for 1 h, the cells were exposed to 2.5 μM MG132 for 11 h and the final 4 h was incubated with MTT. As shown in Fig. 8A, SP600125 failed to suppress the cytotoxicity of MG132, whereas SB202190 at a concentration of 50 μM could reduce the cytotoxicity by up to ~85%. Since it has been reported that ER stress-mediated activation of IRE1α/ASK1/p38MAPK signaling pathway leads to Bak activation and subsequent mitochondrial damage [14], we decided to investigate the effect of p38MAPK inhibitor on MG132-induced $\Delta\psi m$ loss and Bak activation. Although apoptotic sub-G_1 peak was barely or not detectable in continuously growing Jurkat T cells, it increased to the level of 43.1% following treatment with 2.5 μM MG132 for 11 h (Fig. 8B). In the presence of 50 μM SB202190, however, the MG132-induced apoptotic sub-G_1 cells appeared to be 17.6%, indicating that MG132-induced apoptotic cell death was significantly reduced by the p38MAPK inhibitor SB202190. Under the same conditions, both MG132-induced $\Delta\psi m$ loss and Bak activation were also prevented by SB202190 (Fig. 8C and D). These results suggested that ER stress-mediated activation of p38MAPK rather than JNK was involved in Bak activation causing mitochondrial damage during MG132-induced apoptosis.

3.5. Effect of $p56^{lck}$ on MG132-induced cytotoxicity, and apoptotic events in Jurkat T cells

Previously it has been shown that the pro-apoptotic role of $p56^{lck}$ in apoptosis induced by various apoptotic conditions

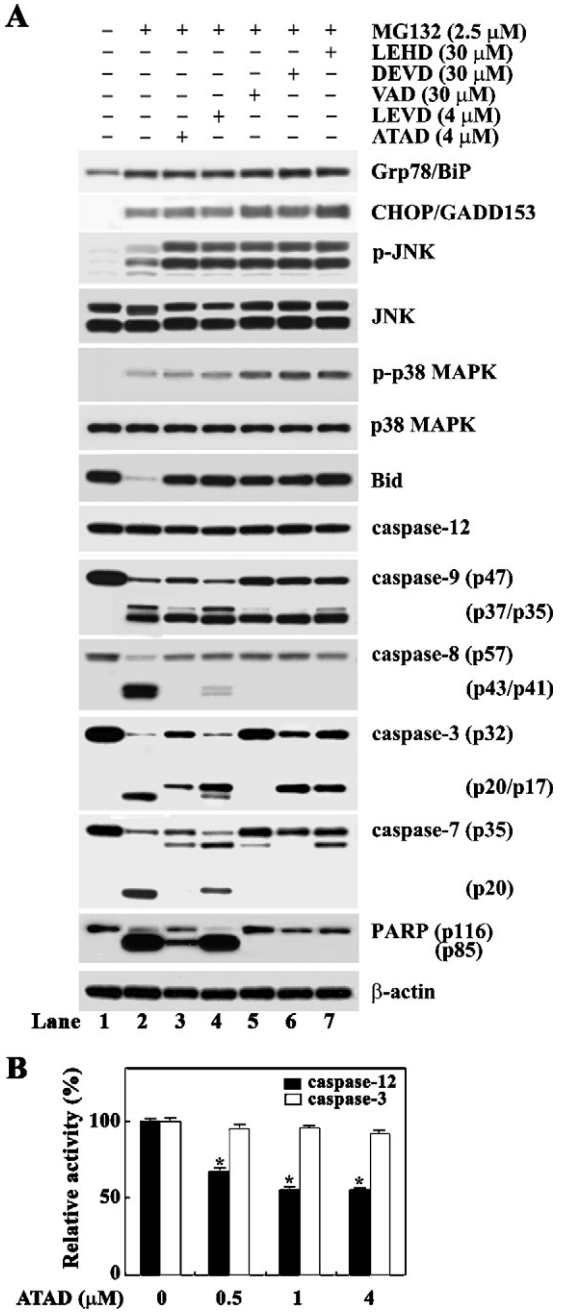

Fig. 7. Western blot analysis of Grp78/BiP, CHOP/GADD153, phospho-JNK, JNK1, phospho-p38MAPK, p38MAPK, Bid, caspase-12, -9, -3, -8, and -7, Bid, cleavage of PARP, and β-actin in Jurkat T cells (clone E6.1) after treatment with 2.5 μM MG132 in the presence of 30 μM z-LEHD-fmk, 30 μM z-DEVD-fmk, 30 μM z-VAD-fmk, 4 μM z-LEVD-fmk, or 4 μM z-ATAD-fmk (A), and inhibitory effect of z-ATAD-fmk on *in vitro* caspase-12 and -3 activities (B). The cells (5×10^5/ml) were preincubated with the individual caspase inhibitors for 2 h and then treated with 2.5 μM MG132 for 12 h. Western analysis was performed as described in Section 2. For the *in vitro* caspase-12 and -3 inhibition assay, the cell lysates (150 μg) prepared from Jurkat T cells treated with 2.5 μM MG132 for 12 h were preincubated with indicated concentrations of z-ATAD-fmk for 30 min, and then the residual caspase-12 activity or caspase-3 activity was assayed as described in Section 2. Each value is expressed as mean ± SD ($n = 3$ with three replicates per independent experiment). *$P < 0.05$ compared to control.

appears to be associated with positively modulating mitochondrial damage [19–23]. However, there has been no report on the effect of $p56^{lck}$ on ER stress-mediated apoptosis. To examine whether MG132-induced apoptosis via the ER stress-mediated apoptotic signaling pathways can be modulated by a Src-family protein tyrosine kinase $p56^{lck}$, the MG132-induced cytotoxicity and various apoptotic events including apoptotic DNA fragmentation, apoptotic sub-G_1 cells, and Δψm loss were compared between $p56^{lck}$-stable transfectant JCaM1.6/lck and $p56^{lck}$-deficient JCaM1.6/vector. When JCaM1.6/lck and JCaM1.6/vector were treated with 0.63 μM, 1.25 μM, and 2.5 μM MG132 for 12 h, the cell viability was 87.0%, 59.8%, and 36.0% in JCaM1.6/lck, and 95.5%, 82.2%, and 65.6% in JCaM1.6/vector, respectively (Fig. 9A). Under the same conditions, the apoptotic DNA fragmentation, the ratio of apoptotic sub-G_1 cells, Δψm loss, and the levels of early apoptotic cells stained only with Annexin V-FITC and late apoptotic cells stained with both Annexin V-FITC and PI were more apparent in JCaM1.6/lck than in JCaM1.6/vector, demonstrating the positive-modulatory role of $p56^{lck}$ in MG132-induced apoptosis in Jurkat T cells (Fig. 9B–E). To understand further the mechanisms underlying the positive modulatory role of $p56^{lck}$ in MG132-induced apoptosis, the MG132-induced apoptotic signaling pathways were compared between $p56^{lck}$-stable transfectant JCaM1.6/lck and $p56^{lck}$-deficient JCaM1.6/vector by Western blot analysis. As shown in Fig. 10A, MG132-induced mitochondrial cytochrome *c* release into cytosol was more significant in JCaM1.6/lck than that in JCaM1.6/vector. Although the level of $p56^{lck}$ in JCaM1.6/lck was essentially the same regardless of treatment with MG132 (1.25–2.5 μM) as was its phosphorylation status on either Tyr-394 or Tyr-505 residues, the presence of $p56^{lck}$ was able to potentiate not only ER stress-mediated upregulation in the levels of Grp78/BiP and CHOP/GADD153 and activation of caspase-12, p38MAPK and Bak but also activation of caspase-9, -3, -7, and -8, Bid cleavage, and degradation of PARP (Fig. 10B–D). In relation to MG132-induced mitochondrial damage, the alteration in the expression levels of Bcl-2 family proteins, including the pro-apoptotic Bcl-2 proteins (Bad, Bak, Bax and Bim), the anti-apoptotic Bcl-2 proteins (Bcl-2 and Bcl-xL), and the anti-apoptotic protein BAG3, were compared between JCaM1.6/lck and JCaM1.6/vector by Western blot analysis. The expression levels of Bad, Bak, and Bax appeared to be higher in JCaM1.6/vector than in JCaM1.6/lck, whereas the expression level of Bcl-xL was similar between JCaM1.6/lck and JCaM1.6/vector, and the expression levels of Bcl-2 and BAG3 were more dominant in JCaM1.6/lck, regardless of MG132 treatment (Fig. 10E). This indicated that the pro-apoptotic effect of $p56^{lck}$ on MG132-induced apoptosis in Jurkat T cells was not due to alteration in the expression profiles of anti-apoptotic and pro-apoptotic Bcl-2 family proteins, because $p56^{lck}$-deficient JCaM1.6/vector as compared to $p56^{lck}$-positive JCaM1.6/lck was likely to possess higher susceptibility to mitochondria-dependent apoptosis. Since ER stress-mediated upregulation in the level of Grp78/BiP and CHOP/GADD153, and activation of p38MAPK and caspase-12 occurred more dominantly in the presence of $p56^{lck}$, these results also indicated that the pro-apoptotic effect of 56^{lck} on MG132-induced apoptosis was attributable to the potentiation of the ER stress-mediated apoptotic events, which could then enhance Δψm loss and mitochondria-dependent activation of caspase cascade. However, a direct blocking of $p56^{lck}$ kinase activity by the Src-like kinase inhibitor PP2 was unable to suppress the MG132-induced cytotoxicity, suggesting that the pro-apoptotic role of $p56^{lck}$ in MG132-induced apoptosis was not mediated by its kinase activity (Fig. 11). Consequently, current results indicated that although the presence of $p56^{lck}$ was not a prerequisite for MG132-induced apoptotic cell death in Jurkat T cells, it could positively modulate the apoptotic cell death by augmenting ER stress-mediated apoptotic events including activation of caspase-12 and p38MAPK, and subsequent activation of Bak and mitochondria-dependent caspase cascade.

4. Discussion

This is the first report to demonstrate that proteasome inhibitor MG132-induced apoptosis can be augmented in the presence of

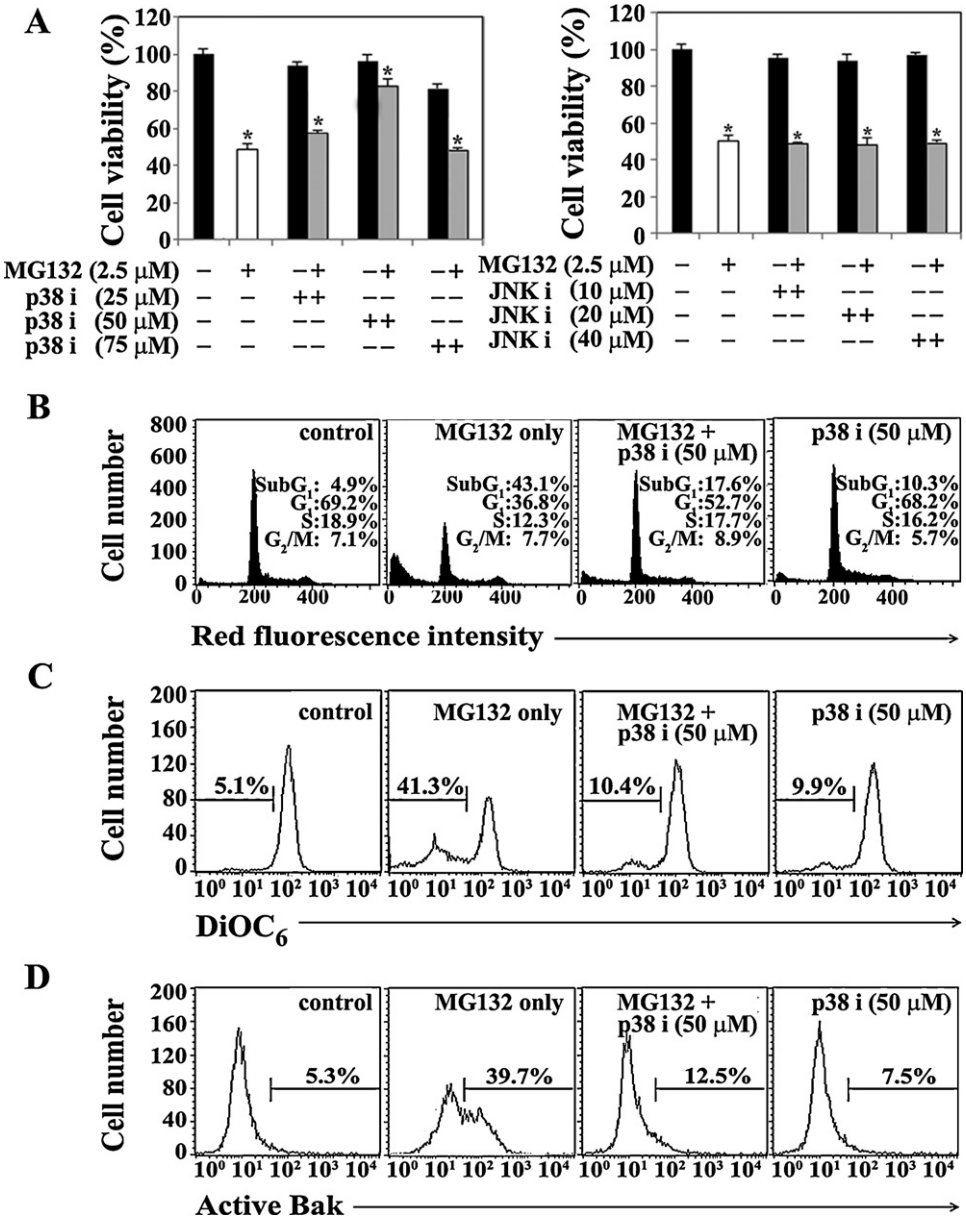

Fig. 8. Suppressive effect of p38MAPK inhibitor (SB202190) or JNK inhibitor (SP600125) on MG132-induced cytotoxicity (A), apoptotic sub-G_1 peak (B), $\Delta\psi$m loss (C), and Bak activation (D) in Jurkat T cells (clone J/Neo). After pretreatment of individual concentrations of SB202190 or SP600125 for 1 h, the treated and untreated cells were incubated with 2.5 μM MG132 at a density of 7.5×10^4/well in a 96-well plate. After 7 h, an MTT assay was performed to determine cell viability. Each value is expressed as mean ± SD ($n = 3$ with three replicates per independent experiment). $^*P < 0.05$ compared to control. Equivalent cultures were prepared, and the cell cycle distribution and the $\Delta\psi$m loss were determined by flow cytometric analysis of PI staining and $DiOC_6$ staining, respectively. Flow cytometric analysis of Bak activation was performed as described in Section 2.

the protein tyrosine kinase $p56^{lck}$ through enhancing the ER stress-mediated activation of caspase-12 and p38MAPK in human acute leukemia Jurkat T cells. No involvement of necrosis in MG132-induced apoptosis of Jurkat T cells as well as its augmentation by $p56^{lck}$ was evidenced by flow cytometric analysis of the cells stained with Annexin V-FITC and PI. In MG132-induced apoptosis of Jurkat T cells, we could exclude an involvement of the extrinsic apoptotic pathway triggered by the Fas/FasL system, because the sensitivity of FADD- and caspase-8-positive wild-type Jurkat clone A3 to the cytotoxicity of MG132 was similar to that of FADD-deficient Jurkat clone I2.1 or caspase-8-deficient Jurkat clone I9.2. Although several studies have reported that the pro-apoptotic roles of $p56^{lck}$ in apoptosis induced either by a physicotherapeutic agent such as ionizing radiation or by chemotherapeutic agents including ceramide, rosmarinic acid, doxorubicin, paclitaxel, 5-fluorouracil, etoposide, and staurosporine are associated with its acting on the mitochondrial apoptotic pathway [19–23], it remains unclear that whether $p56^{lck}$ modulates ER stress-mediated apoptotic signaling. When the newly synthesized proteins are not properly folded and modified before exiting from the ER in cells, the ER lumen becomes accumulated with misfolded or unfolded proteins, which leads to the induction of ER stress. The ER stress activates the unfolded protein response (UPR) to restore a favorable folding environment via not only upregulation of the level of chaperone genes such as Grp78/BiP, calnexin, and calreticulin, which are involved in protein folding in the ER but also activation of the ER-associated degradation (ERAD) system which degrades the misfolded or unfolded proteins in a proteasome-dependent manner [12,13]. However, if the induction of these UPRs fails to overcome the accumulation of misfolded or

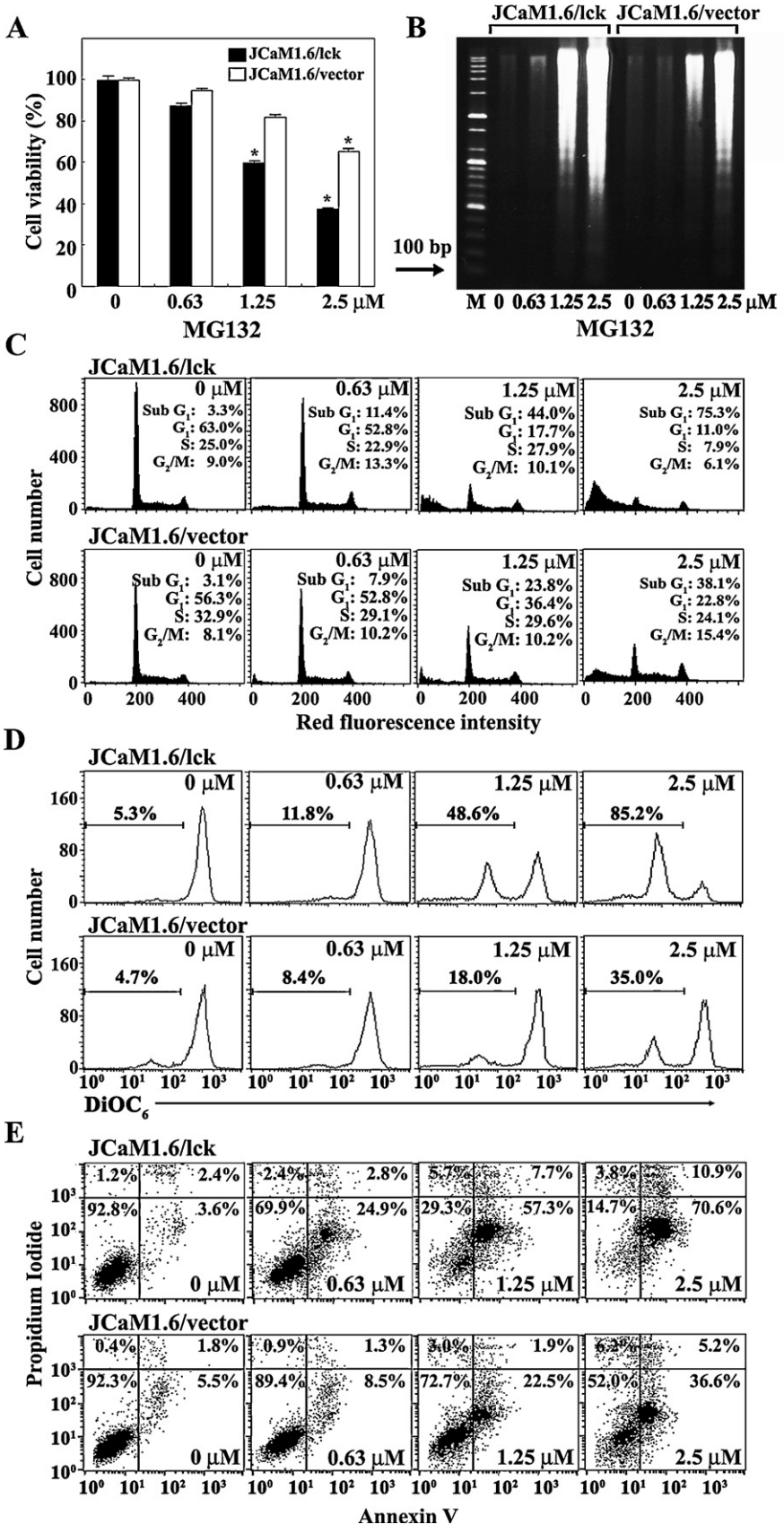

Fig. 9. Effect of MG132 on cell viability (A), apoptotic DNA fragmentation (B), cell cycle distribution (C), $\Delta\psi$m loss (D), and apoptotic cell death (E) in p56^{lck}-stable transfectant JCaM1.6/lck and p56^{lck}-deficient JCaM1.6/vector. Individual cells (7.5×10^4) were incubated with indicated concentrations of MG132 in a 96-well plate for 12 h and the final 4 h were incubated with MTT to determine cell viability. Each value is expressed as mean ± SD ($n = 3$ with three replicates per independent experiment). *$P < 0.05$ compared to control. Equivalent cultures were prepared and processed for apoptotic DNA fragmentation analysis by Triton X-100 lysis methods using 1.2% agarose gel electrophoresis. The cell cycle distribution was determined on an equal number of cells (2×10^4) by flow cytometric analysis of PI staining. The $\Delta\psi$m loss and the apoptotic cells were determined by flow cytometric analysis of $DiOC_6$ staining, and Annexin V-FITC and PI staining, respectively.

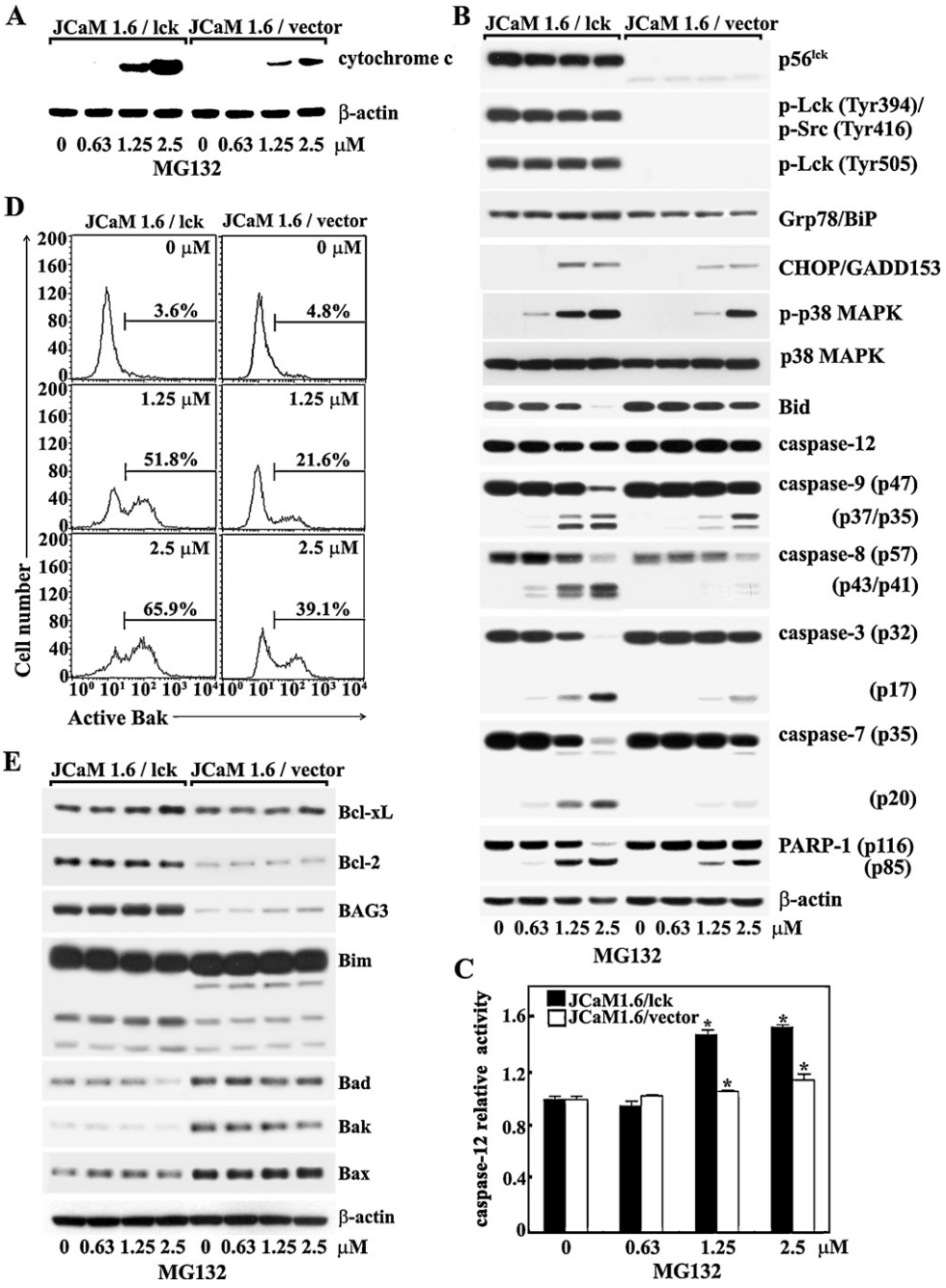

Fig. 10. Western blot analysis of cytochrome *c* release and β-actin (A), $p56^{lck}$, phospho-$p56^{lck}$ (Tyr-394), phospho-$p56^{lck}$ (Tyr-505), Grp78/BiP, CHOP/GADD153, phospho-p38MAPK, p38MAPK, Bid, caspase-12, -9, -8, -3, and -7 activation, PARP cleavage, and β-actin (B), pro-apoptotic Bcl-2 proteins (Bad, Bak, Bax, and Bim), anti-apoptotic Bcl-2 proteins (Bcl-xL and Bcl-2), anti-apoptotic protein BAG3, and β-actin (E), flow cytometric analysis of Bak activation (D), and *in vitro* activity assay for caspase-12 and -3 (C) in $p56^{lck}$-stable transfectant JCaM1.6/lck and $p56^{lck}$-deficient JCaM1.6/vector after treatment with MG132. The cells ($\sim 5 \times 10^6$ cells) were incubated with the indicated concentrations of MG132 for 12 h and prepared for the cell lysates. Western blot analysis, flow cytometric analysis of Bak activation, and the enzymic activity assay of caspase-12 or caspase-3 were performed as described in Section 2. Each value is expressed as mean ± SD ($n = 3$ with three replicates per independent experiment). $^*P < 0.05$ compared to control.

unfolded proteins in the ER, and thus imposes excessive and prolonged stresses, the UPR activates cell destructive pathways, leading to apoptotic cell death [14,30]. At least four death-signaling pathways are known to be involved in this apoptotic event; the first is transcriptional activation of the gene for CHOP/GADD153, a transcription factor potentiating apoptosis [30], the second is activation of JNK/p38MAPK pathway leading to Bak/Bax activation [14,31,34], the third is activation of caspase-8 [32], and the fourth is ER stress-associated activation of caspase-12 [33,50,51]. In these contexts, we investigated if MG132-induced apoptosis in Jurkat T cells was accompanied by upregulation in the levels of Grp78/BiP and CHOP/GADD153 and activation of JNK, p38MAPK, caspase-12 and -8. In accordance with previous studies demonstrating that ER stress-mediated activation of JNK/p38MAPK was upstream of mitochondrial cytochrome *c* release [14,31,34], the activation of JNK and p38MAPK was observed in Jurkat T cells treated with 1.25–2.5 μM MG132. At the same time, the N-terminal conformational change of Bak, representing its activation, was detected by flow cytometric analysis using the conformation-specific anti-Bak (Ab-1). Previously, it has been

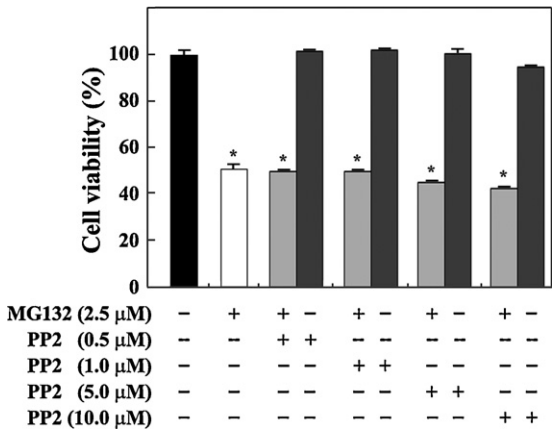

Fig. 11. Effect of the Src-like kinase inhibitor PP2 on MG132-induced cytotoxicity in Jurkat T cells (clone J/Neo). The cells were preincubated with the indicated concentrations of PP2 for 1 h, and then treated with 2.5 μM MG132 at a density of 7.5×10^4/well in a 96-well plate. After 7 h, an MTT assay was performed to assess cell viability. Each value is expressed as mean ± SD ($n = 3$ with three replicates per independent experiment). $^*P < 0.05$ compared to control.

shown that in stress-induced cell death, p38MAPK causes Bak and Bax activation, while JNK causes Bim activation, followed by their translocation to mitochondria [52]. However, neither Bax activation nor Bim activation was detected during MG132-induced cell death of Jurkat T cells (data not shown). In addition, a slight decrease in the level of procaspase-12 (55 kDa) as well as an enhancement in the level of *in vitro* caspase-12 activity was detected, demonstrating MG132-induced activation of caspase-12. Since the active caspase-12 could directly activate procaspase-9 independently of both the mitochondrial cytochrome *c* and Apaf-1 [33], and since the activation of caspase-9 within apoptosome and subsequent activation of caspase-3 were reported to occur through reciprocal activation of caspase-9 and -3 [46–49], these previous and current results indicated that the caspase-12 activation occurred in parallel with mitochondrial cytochrome *c* release in order to synergize the caspase-3 activation targeted by the apoptosome. In addition to activation of JNK, p38MAPK, and caspase-12, caspase-8 activation was also detected in Jurkat T cells following exposure to MG132 (1.25–2.5 μM). A proposed mechanism underlying contribution of ER stress-mediated activation of caspase-8 to mitochondria-dependent caspase cascade is that the active caspase-8 cleaves the Bid protein (26 kDa) into a truncated form, tBid (15 kDa) that is known to target mitochondria in order to mediate cytochrome *c* release into cytosol [36,37]. Although the generation of tBid was not observed by Western blot analysis in the cells treated with MG132, presumably due to the short half-life of tBid, a decrease in the level of Bid protein was detected in accordance with caspase-8 activation and mitochondrial cytochrome *c* release. Consequently, these results suggested that MG132-induced cytochrome *c* release might be initiated through Bak activation by p38MAPK and/or through Bid cleavage into tBid by casapse-8. However, it cannot be excluded that the MG132-induced activation of caspase-8 was not the initial signal generating mitochondrial cytochrome *c* release, but was downstream of the caspase-3 activation, because caspase-8 was previously activated downstream of caspase-3 to comprise a positive feedback loop involving tBid-mediated mitochondrial cytochrome *c* release in the chemical agent-induced apoptosis of tumor cells [53]. While MG132-induced activation of caspase-12, -8, and Bak, mitochondrial cytochrome *c* release and subsequent activation of caspase cascade including caspase-9, -3, and -7, and PARP degradation were completely abrogated in J/Bcl-xL cells overexpressing Bcl-xL, the ER stress-mediated upregulation of Grp78/BiP and CHOP/GADD153 levels, and activation of JNK and p38MAPK appeared to be sustained or modestly enhanced. This suggested that among the MG132-induced apoptotic events mediated via ER stress, the activation of caspase-12 and -8 was sensitive to anti-apoptotic role of Bcl-xL as was the activation of mitochondria-dependent caspase cascade. In addition, these results demonstrated that MG132-induced activation of mitochondria-dependent caspase cascade, which could be blocked by Bcl-xL, was crucial for the induced apoptosis.

Although the presence of the pan-caspase inhibitor z-VAD-fmk completely blocked MG132-induced sub-G_1 peak and most apoptotic events such as activation of caspase-3, -7, and -8, it failed to completely block activation of caspase-9, in particular the generation of 35 kDa active caspase-9. The presence of z-VAD-fmk also failed to suppress MG132-induced JNK and p38MAPK activation and $\Delta\psi m$ loss. Since the active JNK and p38MAPK can trigger mitochondrial cytochrome *c* release [14,31,34,52], and since the proteolytic cleavage of 47 kDa procaspase-9 within the apoptosome appears to yield mainly 35/12 kDa active forms unless the feedback cleavage of 47 kDa procaspase-9 by 20 kDa active caspase-3 occurs [46–49], it was likely that MG132-induced mitochondrial cytochrome *c* release might be initiated by JNK and/or p38MAPK rather than tBid generated from the caspase-8-dependent cleavage of Bid. The notion that caspase-8 activation driven by 17 kDa active caspase-3 was a feedback amplification mechanism promoting mitochondrial cytochrome *c* release via the action of tBid became more evident by our data showing that either the inhibition of caspase-9 activity by z-LEHD-fmk or the inhibition of caspase-3 activity by z-DEVD-fmk could completely block MG132-induced activation of caspase-8 as well as generation of active caspase-3 (17 kDa). While 37 kDa active caspase-9 was barely detected at in the presence of z-LEHD-fmk or z-DEVD-fmk, 35 kDa active caspase-9 was detected at a comparable level to that of the MG132-treated control cells. Under these conditions, only 20 kDa active caspase-3 was generated without inducing caspase-7 activation and PARP degradation. These results also confirmed that the reciprocal activation of caspase-9 and -3 downstream of mitochondrial cytochrome *c* release, which could generate two forms (37/35 kDa) of active caspase-9 and 17 kDa active caspase-3, was critical for MG132-induced activation of caspase-8 and -7 and degradation of PARP. It is noteworthy that human caspase-4, which has a CARD pro-domain like human caspase-12 at the N-terminal and shows a high similarity to mouse caspase-12, has been proposed to play a role in the ER stress-mediated apoptosis of human cells [54]. In this context, the effect of the caspase-12 inhibitor z-ATAD-fmk or the caspase-4 inhibitor z-LEVD-fmk on MG132-induced apoptotic events was investigated. In the presence of z-ATAD-fmk (4 μM), MG132-induced apoptotic sub-G_1 peak, activation of caspase-8 and -7, and degradation of PARP were completely abrogated, whereas generation of 35 kDa active caspase-9 and proteolytic cleavage of procaspase-3 into 19 kDa active form without 17 kDa active form were detected. In contrast, z-LEVD-fmk (4 μM) failed to suppress MG132-induced sub-G_1 peak, activation of caspase-9, and degradation of PARP, although there was a remarkable decrease in activation of caspase-3 generating 17 kDa active form and activation of caspase-8. Since 17 kDa active form was more efficient rather than the 20 kDa active form of caspase-3 in exerting the pro-apoptotic effects including activation of caspase-8 and degradation of PARP [55,56], the current results indicated that when the caspase-12 activity was inhibited by z-ATAD-fmk, the mitochondria-dependent activation of caspase-9 and -3 was not provoked to a sufficient level required for subsequent activation of caspase-8 and -7 and degradation of PARP in Jurkat T cells treated with MG132. These results also suggested that the inhibition of caspase-4 activity by z-LEVD-fmk did not interfere with the mitochondria-dependent activation of caspase-9, but did suppress in part the proteolytic cleavage of

procaspase-3 into 17 kDa active form required for the activation of caspase-8. Consequently, these results suggested that ER stress-induced activation of caspase-12 rather than caspase-4 was critical for the mitochondria-dependent activation of caspase-9 and -3, leading to activation of caspase-8 and -7 and degradation of PARP during MG132-induced apoptosis of Jurkat T cells. Recently, by *in vitro* caspase activity assay using recombinant human caspases, it has been reported that the inhibitory modes of six z-peptide-fmk inhibitors (z-YVAD-fmk for caspase-1, z-VDVAD-fmk for caspase-2, z-DEVD-fmk for caspase-3, z-VEID-fmk for caspase-6, z-IETD-fmk for caspase-8, and z-LEHD-fmk for caspase-9) are not specific for their designated caspases [57]. Although these caspase inhibitors are widely used for cell-based assays at concentrations of up to 20–120 μM, the *in vitro* caspase activity assay has shown that the caspase inhibitors possess cross-reactivity toward non-targeted caspases, and each of them cause complete inhibition of caspase-3, -7, and -8 activities at a concentration of 10 μM. In our hands, however, the minimal concentration of z-VAD-fmk, z-LEHD-fmk, or z-DEVD-fmk to completely prevent MG132-induced apoptosis of Jurkat T cells was ~30 μM, whereas the minimal concentration of the caspase-12 inhibitor z-ATAD-fmk to prevent the MG132-induced apoptosis appeared to be ~4 μM (data not shown). Since the *in vitro* caspase-12 activity assay using the cell lysate of Jurkat T cells exposed to MG132 (2.5 μM) for 12 h revealed that z-ATAD-fmk (1–4 μM) could specifically inhibit the caspase-12 activity by ~50%, it was likely that the inhibitory effect of z-ATAD-fmk (4 μM) on the MG132-induced apoptotic signaling pathway was exerted by its specific inhibition of caspase-12 activity, confirming the critical role of caspase-12 activated via ER stress in MG132-induced apoptosis in Jurkat T cells. These results also indicated that MG132-induced activation of JNK and p38MAPK, which could be mediated by ER stress, was an upstream event of the mitochondria-dependent activation of caspase cascade. On the other hand, the cytotoxic effect of MG132 was partly inhibited by the p38MAPK inhibitor, but not affected by the JNK inhibitor. Furthermore, the p38MAPK inhibitor could suppress MG132-induced Bak activation and $\Delta\psi m$ loss. These results confirmed that the ER stress-mediated activation of p38MAPK was crucial for Bak activation and resultant mitochondrial damage during MG132-induced apoptosis in Jurkat T cells.

The MG132-induced apoptotic events such as cytotoxicity, apoptotic DNA fragmentation, Bak activation, $\Delta\psi m$ loss, and mitochondrial cytochrome *c* release seemed to be more apparent in $p56^{lck}$-stable transfectant JCaM1.6/lck than in $p56^{lck}$-deficient JCaM1.6/vector, indicating pro-apoptotic contribution of $p56^{lck}$ to MG132-induced apoptosis. The $p56^{lck}$ was previously required for ionizing radiation-, ceramide-, rosmarinic acid, doxorubicin-, paclitaxel-, or 5-fluorouracil-induced apoptosis in order to positively modulate mitochondria-dependent caspase cascade [19–23]. A mechanism responsible for the positive regulatory role of $p56^{lck}$ was proposed to be the transcriptional triggering of the Bak expression as evidenced by that the Bak expression was completely absent in $p56^{lck}$-deficient cells, whereas introduction of $p56^{lck}$ by transfection of the *lck* gene appeared to restore Bak expression and conferred sensitivity to the induced apoptosis [23]. These previous results raised a possibility that the pro-apoptotic effect of $p56^{lck}$ on MG132-induced apoptosis might be exerted by potentiating the mitochondrial apoptosis pathway by controlling Bcl-2 family proteins. However, the expression levels of pro-apoptotic Bcl-2 proteins including Bad, Bax, and Bak in $p56^{lck}$-deficient JCaM1.6/vector were much higher than those in $p56^{lck}$-positive JCaM1.6/lck, whereas the expression levels of anti-apoptotic Bcl-2 proteins such as Bcl-xL and Bcl-2, and the anti-apoptotic protein BAG3 were significantly higher in $p56^{lck}$-positive JCaM1.6/lck than $p56^{lck}$-deficient JCaM1.6/vector. Nonetheless, during MG132-induced apoptosis, not only mitochondria-dependent caspase cascade, which leads to PARP degradation but also ER stress-mediated apoptotic events such as upregulation in the levels of Grp78/BiP and CHOP/GADD153, and activation of p38MAPK and caspase-12 appeared to be more dominant in $p56^{lck}$-positive JCaM1.6/lck than $p56^{lck}$-deficient JCaM1.6/vector. This suggested that the $p56^{lck}$-mediated potentiation of mitochondria-dependent caspase cascade in MG132-induced apoptosis was not due to apoptogenic alteration in the expression levels of Bcl-2 family members, but due to potentiation of ER stress-mediated apoptotic events. It is noteworthy that the pro-apoptotic function of $p56^{lck}$, which could enhance MG132-induced apoptosis, was not exerted by its kinase activity, because the presence of the $p56^{lck}$ inhibitor PP2 failed to prevent MG132-induced cytotoxicity. This was consistent with previous studies showing that the pro-apoptotic role of $p56^{lck}$ required for the mitochondria-dependent apoptosis of Jurkat T cells, which was induced by rosmarinic acid, doxorubicin, paclitaxel, or 5-fluorouracil, was not reduced by the specific inhibitor PP2, suggesting that the pro-apoptotic function of $p56^{lck}$ might not be due to its kinase activity [20,21]. The typical Src-family kinase structure of $p56^{lck}$ is known to be composed of a unique N-terminal attachment site for saturated fatty acid addition, followed by a Src homology 3 (SH3) domain, an SH2 domain, a tyrosine kinase domain (SH1), and a C-terminal negative regulatory domain [58]. While the SH2 and SH3 domains have conventional characteristics and mediate binding to regulatory proteins and possible substrates, the kinase activity is controlled by phosphorylation status of tyrosine residues (Tyr-394 and Tyr-505) in the activation loop [59,60]. Although the current results indicated a contribution of $p56^{lck}$, other than its function as a tyrosine kinase, to the ER stress-mediated apoptotic pathway resulting from an inhibition of proteasome activity by MG132, it remains to be elucidated that whether and/or which SH domains are involved. The SH2 domain might be the primary candidate for the pro-apoptotic function of $p56^{lck}$ in MG132-mediated ER stress, because rosmarinic acid-induced apoptosis, which was mediated via mitochondrial pathway, was dependent on the SH2 domain of $p56^{lck}$ [21].

In summary, current results demonstrated that MG132-induced apoptosis was mediated by activation of JNK and caspase-12 via ER stress and subsequent activation of mitochondria-dependent and -independent caspase cascade including caspase-9, -3, -7, and -8, in which ER stress-mediated activation of caspase-12 was crucial for the reciprocal activation of caspase-9 and -3, leading to PARP degradation. The presence of $p56^{lck}$ could positively modulate the MG132-induced apoptotic cell death via enhancing ER stress-mediated activation of JNK and caspase-12, and subsequent mitochondria-dependent or mitochondria-independent activation of caspase cascade.

Conflict of interest

The authors declare no conflict of interest.

Acknowledgement

This work was supported by the Regional Innovation Center Program (Research Center for Biomedical Resources of Oriental Medicine at Daegu Hanny University) of the Ministry of Commerce, Industry and Energy (RIC-B0009008).

References

[1] Coux O, Tanaka K, Goldberg AL. Structure and functions of the 20S and 26S proteasomes. Annu Rev Biochem 1996;65:801–47.
[2] Glickman MH, Ciechanover A. The ubiquitin–proteasome proteolytic pathway: destruction for the sake of construction. Physiol Rev 2002;82:373–428.
[3] Adams J. The proteasome: a suitable antineoplastic target. Nat Rev Cancer 2004;4:349–60.

[4] Oikawa T, Sasaki T, Nakamura M, Shimamura M, Tanahashi N, Omura S, et al. The proteasome is involved in angiogenesis. Biochem Biophys Res Commun 1998;246:243–8.
[5] Almond JB, Cohen GM. The proteasome: a novel target for cancer chemotherapy. Leukemia 2002;16:433–43.
[6] Miller LA, Goldstein NB, Johannes WU, Walton CH, Fujita M, Norris DA, et al. ABT-737 and a proteasome inhibitor synergistically kill melanomas through Noxa-dependent apoptosis. J Invest Dermatol 2009;129:964–71.
[7] Obeng EA, Carlson LM, Gutman DM, Harrington Jr WJ, Lee KP, Boise LH. Proteasome inhibitors induce a terminal unfolded protein response in multiple myeloma cells. Blood 2006;107:4907–16.
[8] Wagenknecht B, Hermisson M, Groscurth P, Liston P, Krammer PH, Weller M. Proteasome inhibitor-induced apoptosis of glioma cells involves the processing of multiple caspases and cytochrome *c* release. J Neurochem 2000;75:2288–97.
[9] Kitagawa H, Tani E, Ikemoto H, Ozaki I, Nakano A, Omura S. Proteasome inhibitors induce mitochondria-independent apoptosis in human glioma cells. FEBS Lett 1999;443:181–6.
[10] Wang X, Luo H, Chen H, Duguid W, Wu J. Role of proteasomes in T cell activation and proliferation. J Immunol 1998;160:788–801.
[11] Yan XB, Yang DS, Gao X, Feng J, Shi ZL, Ye Z. Caspase-8 dependent osteosarcoma cell apoptosis induced by proteasome inhibitor MG132. Cell Biol Int 2007;31:1136–43.
[12] Meusser B, Hirsch C, Jarosch E, Sommer T. ERAD: the long road to destruction. Nat Cell Biol 2005;7:766–72.
[13] Oyadomari S, Yun C, Fisher EA, Kreglinger N, Kreibich G, Oyadomari M, et al. Cotranslocational degradation protects the stressed endoplasmic reticulum from protein overload. Cell 2006;126:727–39.
[14] Kim I, Shu CW, Xu W, Shiau CW, Grant D, Vasile S, et al. Chemical biology investigation of cell death pathways activated by endoplasmic reticulum stress reveals cytoprotective modulators of ASK1. J Biol Chem 2009;284:1593–603.
[15] Perlmutter RM, Levin SD, Appleby MW, Anderson SJ, Alberola-Ila J. Regulation of lymphocyte function by protein phosphorylation. Annu Rev Immunol 1993;11:451–99.
[16] Marth JD, Peet R, Krebs EG, Perlmutter RM. A lymphocyte-specific protein-tyrosine kinase gene is rearranged and overexpressed in the murine T cell lymphoma LSTRA. Cell 1985;43:393–404.
[17] Eischen CM, Williams BL, Zhang W, Samelson LE, Lynch EH, Abraham RT, et al. ZAP tyrosine kinase is required for the up-regulation of FAS ligand in activation-induced T cell apoptosis. J Immunol 1997;159:1135–9.
[18] Sharif-Askari E, Gaucher D, Halwani R, Ma J, Jao K, Abdallah A, et al. $p56^{Lck}$ tyrosine kinase enhances the assembly of death-inducing signaling complex during Fas-mediated apoptosis. J Biol Chem 2007;282:36048–56.
[19] Belka C, Marini P, Lepple-Wienhues A, Budach W, Jekle A, Los M, et al. The tyrosine kinase lck is required for CD95-independent caspase-8 activation and apoptosis in response to ionizing radiation. Oncogene 1999;18:4983–92.
[20] Gruber C, Henkel M, Budach W, Belka C, Jendrossek V. Involvement of tyrosine kinase p56/Lck in apoptosis induction by anticancer drugs. Biochem Pharmacol 2004;67:1859–72.
[21] Hur YG, Yun Y, Won J. Rosmarinic acid induces $p56^{lck}$-dependent apoptosis in Jurkat and peripheral T cells via mitochondrial pathway independent from Fas/Fas ligand interaction. J Immunol 2004;172:79–87.
[22] Manna SK, Sah NK, Aggarwal BB. Protein tyrosine kinase $p56^{lck}$ is required for ceramide-induced but not tumor necrosis factor-induced activation of NF-kappa B, AP-1, JNK, and apoptosis. J Biol Chem 2000;275:13297–306.
[23] Samraj AK, Stroh C, Fischer U, Schulze-Osthoff K. The tyrosine kinase Lck is a positive regulator of the mitochondrial apoptosis pathway by controlling Bak expression. Oncogene 2006;25:186–97.
[24] Al-Ramadi BK, Zhang H, Bothwell ALM. Cell-cycle arrest and apoptosis hypersusceptibility as a consequence of Lck deficiency in nontransformed T lymphocytes. Proc Natl Acad Sci USA 1998;95:12498–503.
[25] Park HS, Jun DY, Han CR, Kim YH. Protein tyrosine kinase $p56^{lck}$-deficiency confers hypersusceptibility to p-fluorophenylalanine (pFPhe)-induced apoptosis by augmenting mitochondrial apoptotic pathway in human Jurkat T cells. Biochem Biophys Res Commun 2008;377:280–5.
[26] Jun DY, Rue SW, Han KH, Taub D, Lee YS, Bae YS, et al. Mechanism underlying cytotoxicity of thialysine, lysine analog, toward human acute leukemia Jurkat T cells. Biochem Pharmacol 2003;66:2291–300.
[27] Jun DY, Kim JS, Park HS, Han CR, Fang Z, Woo MH, et al. Apoptogenic activity of auraptene of *Zanthoxylum schinifolium* toward human acute leukemia Jurkat T cells is associated with ER stress-mediated caspase-8 activation that stimulates mitochondria-dependent or -independent caspase cascade. Carcinogenesis 2007;28:1303–13.
[28] Zamzami N, Marchetti P, Castedo M, Zanin C, Vayssière JL, Petit PX, et al. Reduction in mitochondrial potential constitutes an early irreversible step of programmed lymphocyte death in vivo. J Exp Med 1995;181:1661–72.
[29] Kim SM, Park HS, Jun DY, Woo HJ, Woo MH, Yang CH, et al. Mollugin induces apoptosis in human Jurkat T cells through endoplasmic reticulum stress-mediated activation of JNK and caspase-12 and subsequent activation of mitochondria-dependent caspase cascade regulated by Bcl-xL. Toxicol Appl Pharmacol 2009;241:210–20.
[30] Lai E, Teodoro T, Volchuk A. Endoplasmic reticulum stress: signaling the unfolded protein response. Physiology 2007;22:193–201.
[31] Aoki H, Kang PM, Hampe J, Yoshimura K, Noma T, Matsuzaki M, et al. Direct activation of mitochondrial apoptosis machinery by c-Jun N-terminal kinase in adult cardiac myocytes. J Biol Chem 2002;277:10244–50.
[32] Jimbo A, Fujita E, Kouroku Y, Ohnishi J, Inohara N, Kuida K, et al. ER stress induces caspase-8 activation, stimulating cytochrome *c* release and caspase-9 activation. Exp Cell Res 2003;283:156–66.
[33] Rao RV, Castro-Obregon S, Frankowski H, Schuler M, Stoka V, del Rio G, et al. Coupling endoplasmic reticulum stress to the cell death program; an Apaf-1-independent intrinsic pathway. J Biol Chem 2002;277:21836–42.
[34] Urano F, Wang X, Bertolotti A, Zhang Y, Chung P, Harding HP, et al. Coupling of stress in the ER to activation of JNK protein kinases by transmembrane protein kinase IRE1. Science 2000;287:664–6.
[35] Davis RL. Signal transduction by the JNK group of MAP kinases. Cell 2000;103:239–52.
[36] Li H, Zhu H, Xu C, Yuan J. Cleavage of Bid by caspase-8 mediates the mitochondrial damage in the Fas pathway of apoptosis. Cell 1998;94:491–501.
[37] Desagher S, Osen-Sand A, Nichols A, Eskes R, Montessuit S, Lauper S, et al. Bid-induced conformational change of Bax is responsible for mitochondrial cytochrome *c* release during apoptosis. J Cell Biol 1999;144:891–901.
[38] Juo P, Woo MS, Kuo CJ, Signorelli P, Biemann HP, Hannun YA, et al. FADD is required for multiple signaling events downstream of the receptor Fas. Cell Growth Differ 1999;10:797–804.
[39] Anto RJ, Mukhopadhyay A, Denning K, Aggarwal BB. Curcumin (diferuloylmethane) induces apoptosis through activation of caspase-8, BID cleavage and cytochrome *c* release: its suppression by ectopic expression of Bcl-2 and Bcl-xL. Carcinogenesis 2002;23:143–50.
[40] Kluck RM, Bossy-Wetzel E, Green DR, Newmeyer DD. The release of cytochrome *c* from mitochondria: a primary site for Bcl-2 regulation of apoptosis. Science 1997;275:1132–6.
[41] Ozoren N, Kim KH, Burns TF, Dicker DT, Moscioni AD, El-Deiry WS. The caspase-9 inhibitor Z-LEHD-FMK protects human liver cells while permitting death of cancer cells exposed to tumor necrosis factor-related apoptosis-inducing ligand. Cancer Res 2009;60:6259–65.
[42] Barut S, Unlü YA, Karaoğlan A, Tunçdemir M, Dağistanli FK, Oztürk M, et al. The neuroprotective effects of z-DEVD.fmk, a caspase-3 inhibitor, on traumatic spinal cord injury in rats. Surg Neurol 2005;64(3):213–20.
[43] Slee EA, Zhu H, Chow SC, MacFarlane M, Nicholson DW, Cohen GM. Benzyloxycarbonyl-Val-Ala-Asp (OMe) fluoromethylketone (z-VAD-fmk) inhibits apoptosis by blocking the processing CPP32. Biochem J 1996;315:21–4.
[44] Jiang CC, Chen LH, Gillespie S, Wang YF, Kiejda KA, Zhang XD, et al. Inhibition of MEK sensitizes human melanoma cells to endoplasmic reticulum stress-induced apoptosis. Cancer Res 2007;67:9750–61.
[45] Yang SH, Chien CM, Chang LS, Lin SR. Cardiotoxin III-induced apoptosis is mediated by Ca^{2+}-dependent caspase-12 activation in K562 cells. J Biochem Mol Toxicol 2008;22:209–18.
[46] Denault JB, Eckelman BP, Shin H, Pop C, Salvesen GS. Caspase 3 attenuates XIAP (X-linked inhibitor of apoptosis protein)-mediated inhibition of caspase 9. Biochem J 2007;405:11–9.
[47] Fujita E, Egashira J, Urase K, Kuida K, Momoi T. Caspase-9 processing by caspase-3 via a feedback amplification loop in vivo. Cell Death Differ 2001;8:335–44.
[48] Twiddy D, Cain K. Caspase-9 cleavage, do you need it? Biochem J 2007;405:e1–2.
[49] Zou H, Yang R, Hao J, Wang J, Sun C, Fesik SW, et al. Regulation of the Apaf-1/caspase-9 apoptosome by caspase-3 and XIAP. J Biol Chem 2003;278:8091–8.
[50] Nakagawa T, Yuan J. Cross-talk between two cysteine protease families; activation of caspase-12 by calpain in apoptosis. J Cell Biol 2000;150:887–94.
[51] Nakagawa T, Zhu H, Morishima N, Li E, Xu J, Yankner BA, et al. Caspase-12 mediates endoplasmic reticulum-specific apoptosis and cytotoxicity by amyloid-beta. Nature 2000;403:98–103.
[52] Chen CL, Lin CF, Chang WT, Huang WC, Teng CF, Lin YS. Ceramide induces p38 MAPK and JNK activation through a mechanism involving a thioredoxin-interacting protein-mediated pathway. Blood 2008;111:4365–74.
[53] Tang D, Lahti JM, Kidd VJ. Caspase-8 activation and bid cleavage contribute to MCF7 cellular execution in a caspase-3-dependent manner during staurosporine-mediated apoptosis. J Biol Chem 2000;275:9303–7.
[54] Momoi T. Caspases involved in ER stress-mediated cell death. J Chem Neuroanat 2004;28:101–5.
[55] Desagher S, Martinou JC. Mitochondria as the central control point of apoptosis. Trends Cell Biol 2000;10:369–77.
[56] Han Z, Hendrickson EA, Bremner TA, Wyche JH. A sequential two-step mechanism for the production of the mature p17:p12 form of caspase-3 in vitro. J Biol Chem 1997;272:13432–6.
[57] Pereira NA, Song Z. Some commonly used caspase substrates and inhibitors lack the specificity required to monitor individual caspase activity. Biochem Biophys Res Commun 2008;377:873–7.
[58] Palacios EH, Weiss A. Function of the Src-family kinases, Lck and Fyn, in T-cell development and activation. Oncogene 2004;23:7990–8000.
[59] Gervais FG, Chow LM, Lee JM, Branton PE, Veillette A. The SH2 domain is required for stable phosphorylation of $p56^{lck}$ at tyrosine 505, the negative regulatory site. Mol Cell Biol 1993;13:7112–21.
[60] Mustelin T, Tasken K. Positive and negative regulation of T-cell activation through kinases and phosphatases. Biochem J 2003;371:15–27.